Sopok

AIAA 95-2440

UNIFIED COMPUTER MODEL FOR PREDICTING THERMOCHEMICAL EROSION IN GUN BARRELS

Dunn, Stuart, Coats, Douglas, and Nickerson, Gary
Software and Engineering Associates, Inc.
Carson City, Nevada 89701

Sopok, Samuel, O'Hara, Peter, and Pflegl, George
US Army Benet Laboratories
Watervliet, New York 12189

31st AIAA/ASME/SAE/ASEE
Joint Propulsion Conference and Exhibit
July 10-12, 1995/San Diego, CA

UNIFIED COMPUTER MODEL FOR PREDICTING THERMOCHEMICAL EROSION IN GUN BARRELS

Stuart Dunn[a], Samuel Sopok[b], Douglas Coats[a],
Peter O'Hara[b], Gary Nickerson[a], and George Pflegl[b]

[a]Software and Engineering Associates, Inc.,
Carson City, Nevada 89701
(702-882-1966, stu@seainc.com)

[b]US Army Benet Laboratories,
Watervliet, New York 12189
(518-266-4952, ssopok@pica.army.mil)

ABSTRACT

The first known gun barrel thermochemical erosion modeling code is presented. This modeling code provides the necessary missing element needed for developing a generalized gun barrel erosion modeling code that can provide analysis and design information that is unattainable by experiment alone. At the current stage of code development, single-shot comparisons can be made of either the same gun wall material for different rounds or different gun wall materials for the same round. This complex computer analysis is based on rigorous scientific thermochemical erosion considerations that have been validated in the reentry nosetip and rocket nozzle community over the last forty years. The 155-mm M203 Unicannon system example is used to illustrate the five module analyses for chromium and gun steel wall materials for the same round. The first two modules include the standard gun community interior ballistics (XNOVAKTC) and nonideal gas thermochemical equilibrium (BLAKE) codes. The last three modules, significantly modified for gun barrels, include the standard rocket community mass addition boundary layer (TDK/MABL), gas-wall chemistry (TDK/ODE), and wall material ablation conduction erosion (MACE) codes. These five module analyses provide recession, temperature, and heat flux profiles for each material as a function of time and axial position. In addition, this output can be coupled to FEA cracking codes. At the peak heat load axial position, predicted single-shot thermochemical wall erosion showed uncracked gun steel eroded by a factor of one hundred million more than uncracked chromium. For chromium plated gun steel, with its associated crack profile, it appears that gun steel ablation at the chromium cracks leaves unsupported chromium, which is subsequently removed by the high-speed gas flow.

INTRODUCTION

The field of aerothermochemistry, the study of chemical reactions in flow systems, was first described by von Karman in 1951[1]. He introduced a fundamental approach to laminar flame initiation, propagation, and combustion in and around sonic and hypersonic boundary layers with reacting chemical flows.

The modification of the heat transfer coefficient by a blocking effect for the mass addition of chemically reacting wall material into the boundary layer was first described by Reshotko and Cohen in 1955[2,3].

The thermochemical erosion of reentry vehicle (RV) heat shield material for various chemically reacting systems was first studied by Denison and Dooley in 1957[4]. Reentry vehicles experience high temperatures and pressures, including nonlinear mass addition boundary layer (blowing) and shocks. The thermal protection system requires subliming or ablating heat shield protection, whereby the increased blowing results in decreased heat

transfer.

Denison and Dooley's analysis regarding convective heat transfer with mass addition and chemical reactions was subsequently unified and summarized by Lees of California Institute of Technology and The Ramo-Wooldridge Corporation in 1958[5]. Lees' paper explained in a fairly straightforward manner the assumptions required to solve the thermochemical erosion problem with the tools available at that time. In fact, the test of time has demonstrated that the major assumptions in Lees' paper are still reasonable and valid. Initially, Lees' thermochemical erosion analysis model was successfully applied to external flows such as RV thermal protection systems (RV nosetips).

Many recently declassified or unclassified experimental and analytical programs in the rocket community were spawned from Lees' work and led to the development of a number of thermochemical ablation and mechanical erosion computer models for predicting RV nosetip performance and recession[6-16].

Later, Lees' thermochemical erosion analysis model was successfully applied to internal flows associated with chemical rocket systems. Although the chemistry associated with rocket engines is considerably different than the RV environment, the analysis techniques were basically the same. Again, Lees' work led to the development of a number of thermochemical ablation and mechanical erosion computer models for predicting rocket chamber/nozzle performance and recession[17-25].

In the last twenty years, gun barrel technology has primarily focused on mechanical and metallurgical aspects with a secondary focus on erosion. Catastrophic gun barrel failures have been nearly eliminated, while thermochemical erosion (thermochemical ablation with mechanical erosion) problems have intensified due to performance requirements demanding the use of high flame temperature propellants. The erosion of gun barrels is generally attributed to both thermal ablation (bore surface melting with aerodynamic flow removal) and chemical ablation (gas-wall chemical interaction with removal of surface material by high-speed flow). If the surface temperature remains below the solidus temperature, as a practical gun design should, the primary erosion mechanism is chemical ablation. If the temperature rises above the solidus temperature, both chemical and thermal ablation contribute to erosion. In 1990, the U.S. Army Benet Laboratories (Benet) Thermal Management Team identified the need for, secured multi-year funding for, and pursued the development of a unified modeling code for predicting thermochemical erosion in gun barrels. An extensive literature search of military, NASA, and commercial sources revealed that there were no "shrink-wrapped" thermochemical erosion modeling codes for gun barrels. This search did reveal the Two-Dimensional Kinetics Nozzle Performance (TDK) (chemistry, mass addition boundary layer (MABL)) and the Materials Ablation Conduction Erosion (MACE) modeling codes that work together to predict thermochemical ablation with mechanical erosion in the rocket chamber, throat, and nozzle[26,27].

Since the dawn of the space-age, the TDK/MACE codes, and their predecessors[7-10,14-25] have been the JANNAF standard for rocket performance and nozzle erosion predictions. Software and Engineering Associates, Inc. (SEA), is now the sole maintainer and developer of these rocket erosion codes. Since SEA is composed of *rocket* people and Benet is composed of *gun* people, it took a half-year to teach each other about the differences between guns and rockets, and mutually determine that these codes actually exceed gun erosion code requirements and expectations[28]. It became obvious that two of the analytical tools needed to begin the thermochemical erosion analysis of gun barrels were already available in the gun community. These tools were Freedman's BLAKE thermodynamic equilibrium code with compressibility[29], and Gough's NOVA interior ballistics code[30]. It took nearly a year and a half to successfully modify the BLAKE, NOVA, TDK, and MACE codes into a unified gun erosion code[31-33].

A joint SEA/Benet research seminar was given at Benet on the BLAKE/NOVA/TDK/MACE gun erosion code to present its capabilities, using Advanced Field Artillery System (AFAS) Unicannon gun system data[34,35].

A joint SEA/Benet training course was given at SEA on the BLAKE/NOVA/TDK/MACE gun erosion code to provide very detailed information on

all aspects of this gun erosion code, including fundamentals, assumptions, module linkage, execution, and parametric engineering analysis using AFAS Unicannon gun system data[36].

It is the intention of this paper to introduce and outline improvements for what is believed to be the first unified thermochemical erosion modeling code for gun barrels based on Lees'[5] thermochemical erosion analysis model for RV heat shields and rockets. Although it was an option, mechanical erosion effects include only high- speed gas flow and not projectile effects. This SEA erosion model is a practical approach based on an engineering model and not on a data-starved Navier-Stokes approach. Future improvements required to complete the analysis are phase-dependent blowing parameters, a time-dependent boundary layer, and a master control module for automation. In addition, this code requires critical propellant-gun system specific information built into an automated data base. Specifically designed Arrhenius and combustion gas analysis testers will provide Arrhenius profiles and combustion gas constituents, respectively. Chemical erosion data will be acquired by examining the thermochemical-mechanical alloy properties, the gas-metal eroded surface products, and the gas-metal effluent products[37-40].

In the absence of system-specific experimental test data, previous general experimental test data can be substituted. Complex chemical interactions exist between a multicomponent gas and a multicomponent alloy because the alloy components have different selective affinities for the reactive gases, and the reactive species may not diffuse at the same rate through the alloy surface scale. In addition, alloy strength is reduced as reactive gases internally dissolve/react in alloys, or an alloy component forms a low melting point oxide that enhances erosion[41,42].

For this 155-mm M203 Unicannon system analysis, it was necessary to use past experimental data already available in the gun community to determine the existence of thermochemical activity, thermochemical Arrhenius profiles, and thermochemical combustion gas constituents. This experimental data showed that thermomechanical effects alone, with a nonreactive (frozen chemistry) gas mixture, do not fully explain the extent of erosion in gun tubes. Therefore, it must be assumed that thermochemical effects are a significant factor. In addition, this data indicates that propellant combustion products and alloy erosion products are gun system-dependent[43,44].

This experimental data shows that although nonequilibrium conditions may exist at the gas-wall interface, equilibrium potentials from the TDK code could be used for the MACE code. This approximation is valid in the oxide scale at the metal/metal oxide and metal oxide/metal oxide interfaces[45,46], since equilibrium exists at the high temperatures and pressures of interest.

This experimental data also shows two distinctly different "chemical-related" gas-wall interactions for typical chemically reducing solid propellant product-steel (or chromium plated steel) systems. The first "chemical-related" gas-wall interaction is the carburization of iron and chromium involving the diffusion of carbon into the metal matrix at peak gun temperatures and pressures. In this case, the carbon forms a solid solution with the iron or chromium. In this region, the metal's structure is unaltered and the metal and the carbon are two distinctly different components in physical proximity, but not chemically bound. This case describes a purely mechanical interaction and does not describe true thermochemical ablation. As the system returns to room temperature, the iron-metal matrix cannot physically retain the free carbon and precipitates "physically bound" carbon as chemically bound iron carbide (Fe_3C) throughout the solid solution iron matrix. The return to room temperature also causes thermal contractions between surface austenite and carburized subsurface tempered martensite, which produces stress cracks ("heat checking"). This carburization effect still does not qualify as thermochemical ablation, since it is not a surface phenomenon and no material has been removed. This interaction is considered an in-depth phenomenon, considering that the metal matrix alloy is "case-hardened," has a lowered melting point, and is weakened due to cracking and mechanical erosive forces. Experimental data supports the existence of gun barrel carburization[47-50]. The melting point of gun steel is 400° C lower than the melting point of chromium. For these systems, carburization lowers the solidus melting point by 50° to 400° C for gun

steel and 50° to 100°C for chromium, based on respective phase diagrams which justify chromium plating of steel.

This experimental data also shows another "chemical-related" gas-wall interaction for typical chemically reducing solid propellant product-steel (or chromium plated steel) systems. This second "chemical-related" gas-wall interaction is the oxidation of iron and chromium. This occurs initially at the metal matrix-gas interface, then at the metal matrix-metal oxide interface. The process involves the diffusion of oxygen from oxygen-rich gas product species into the metal matrix at peak gun temperatures and pressures. In this case, the oxygen forms a distinct iron or chromium oxide scale layer. This case describes true thermochemical ablation, since the brittle scale layer is highly susceptible to cracking and is easily removed by mechanical erosive forces. As the system returns to room temperature, the metal oxide retains the same chemical structure in the scale layer. Despite the possibility of nonequilibrium at the gas-wall interface, experimental data and chemical equilibrium codes indicate the near exclusive presence of iron oxide or chromium oxide metal-gas compound products when exposed to the combustion products. Typically, these chemically reacting gases require approximately a 50 percent increase in molar oxygen to obtain complete product combustion to carbon dioxide and water. Experimental data supports the existence of gun barrel oxidation[51-57]. For these systems, oxidation lowers melting point by 100° to 200°C for gun steel and raises the melting point by 400° to 500°C for chromium, based on respective phase diagrams which further justify chromium plating of steel.

PROCEDURE

The 155-mm M203 Unicannon gun system thermochemical erosion analysis procedure consists of five analyses, utilizing the NOVA, BLAKE, TDK/MABL, TDK/ODE, and MACE codes. Figure 1 outlines the 155-mm M203 bore erosion analysis procedures for the NOVA (interior ballistics analysis), BLAKE (gas thermochemical equilibrium analysis), TDK/MABL (boundary layer mass addition analysis), TDK/ODE (gas-wall thermochemical equilibrium analysis), and MACE (ablation, erosion, and temperature profile analysis) codes.

The NOVA code interior ballistics analysis includes the 6.9 meter cannon with a 0.020 second inbore phase, the M203 charge, the 11.89 kg M30A1 propellant, and the 43.64 kg M549 projectile. The NOVA code calculates the time-dependent flow field, and evaluates the maximum and minimum state variables. The results of the NOVA calculations may be considered the input to the entire erosion analysis. The NOVA input file is given in the Appendix and follows the format given in the NOVA User's Manual[30]. This file contains gun system specific data not included within the NOVA code. NOVA outputs gas pressure (MPa), gas velocity (m/s), gas temperature (°C), and film coefficient (mJ/m*m*s*C) data at the wall. At 12 preselected axial locations, separate files were generated which contained the above data as a function of time. A file generation utility code is used to convert the 12 axial location NOVA output files (with pressure, velocity, temperature, and density versus time) into 12 preselected time slice linkage files (with pressure, velocity, temperature, and density versus axial distance) with the format required by the TDK/MABL analysis module. Although this is an extremely limited sampling, the time factor and the meticulous nature of linking up the different modules necessitate this approach. These files contain boundary layer edge conditions that will be used by the TDK/MABL code to calculate heat transfer parameters.

The BLAKE thermochemical equilibrium analysis evaluates the maximum and minimum state variable ranges identified by the NOVA output. The BLAKE input file is given in the Appendix and follows the format given in the BLAKE User's Manual[29]. This file contains the M30A1 chemistry and state variable ranges. BLAKE was modified to output chemical composition and compressibility (dense gas correction) linkage file data at the 12 axial locations as a function of NOVA temperature and pressure variations. These files were subsequently used to calculate gas properties by the TDK/MABL and TDK/ODE modules.

The TDK/MABL analysis calculates the boundary layer characteristics with the edge properties extracted from the 12 NOVA preselected time slice linkage files (with pressure, velocity, temperature, and density versus axial location) and BLAKE linkage file (chemical composition and compressibility versus

temperature and pressure). The boundary layer module calculates adiabatic conditions and cold wall heat transfer rate, using the above files as input. The TDK/MABL analysis first calculates the adiabatic condition ($q_{hw} = 0$) and then calculates the cold wall condition (T_{wall} and H_{wall} both are constant), resulting in a total of 24 analyses. It should be noted that at this stage of development, TDK/MABL will not tolerate negative velocities and smoothing may be required for some of the above 12 linkage files. The TDK/MABL analysis requires 24 input files (12 adiabatic and 12 cold wall), where each includes chemistry and compressibility for the applicable state variable ranges. Examples of the first adiabatic and first cold wall input files are given in the Appendix and follow the format given in the TDK User's Manual[26]. The TDK/MABL code internally generates transport properties and Mollier gas properties for each analysis, and this data is used to calculate the boundary layer characteristics. TDK/MABL generates 24 output files with adiabatic conditions, and heat transfer rates, which are subsequently used to tabulate time-dependent boundary layer properties at two selected locations, the 1- and 2-foot axial stations.

The TDK/ODE analysis requires eight cases including: (1) nonreacting inert wall with no omitted species; (2) nonreacting inert wall with omitted condensed species, C(GR); (3) reacting chromium wall with no omitted species; (4) reacting chromium wall with omitted species C(GR), $CR_2N(S)$, CRN(S); (5) reacting gun steel wall with no omitted species; (6) reacting gun steel wall with omitted species C(GR); (7) reacting iron wall with no omitted species; and (8) reacting iron wall with omitted species C(GR). All of the above cases include the BLAKE chemical composition and compressibility (versus temperature and pressure) linkage file data. In cases 3 though 8, the solid propellant combustion products are totally saturated with many times the wall material. Product omissions are based on the U.S. Army Watertown Arsenal report[51]. The eight key input files are given in the Appendix and follow the format given in the TDK User's Manual[26]. These files contain the M30A1 chemistry and state variable ranges. For each case, TDK/ODE outputs linkage files (Mollier charts) as a function of pressure and temperature for MACE, including (1) inert gas-wall enthalpy $(H_{gw})_{inert}$ linkage file; (2) reacting gas-wall enthalpy $(H_{gw})_{reacting}$ linkage file; and (3) chemical ablation potential (B_a) linkage file.

The MACE analysis computes the resulting thermochemical erosion response and in-depth temperature profiles. The analysis was performed for four cases, which include two chromium calculations and two gun steel calculations (both at axial locations at 1 foot and 2 feet). The corresponding MACE input files, which follow the format described in the MACE User's Manual[27], are generated from the TDK/MABL and TDK/ODE linkage data described above, and are given in the Appendix. The convective environment section (i.e., pressure, recovery enthalpy, cold wall heat transfer rate, etc.) was varied in the above files. MACE linkage file data from TDK/MABL includes tabulated cold wall heating data, thermal properties, recovery enthalpy data, and transport properties data, from the 24 corresponding TDK/MABL cases. MACE linkage file data from TDK/ODE is in the form of Mollier charts, and includes inert gas-wall enthalpy, reacting gas-wall enthalpy, and the chemical ablation potential for each case. MACE outputs surface erosion, surface temperature, and temperature profiles as a function of time for each case.

RESULTS AND DISCUSSION

The current thermochemical erosion model requires input from five different analyses in order to compute surface recession. As an example, the AFAS 155-mm system including the M203 charge and M30A1 propellant is used. The time-dependent core flow in the gun barrel must be known. That is, the velocity, pressure, and temperature distribution in the barrel must be known as a function of time and space. For our analysis, this information is considered to be a specified input. Next the chemical composition of the gases in the barrel must also be known. Our model is based on the premise that equilibrium chemistry applies at the temperatures and pressures associated with gun barrel interior ballistics. Equilibrium chemistry calculations are made for the combusted propellant without wall material. With the core flow properties known, the boundary layer parameters can be calculated, again assuming chemical equilibrium. As pointed out by Lees[5], the boundary layer analysis can be calculated for a nonreacting wall, and modified to account for chemical reactions and mass addition. Two boundary

layer calculations are necessary for each time point evaluated, the first to calculate the cold wall heat transfer coefficient and the second to calculate the adiabatic wall temperature. Then thermochemical equilibrium chemistry calculations are made with the combusted propellant gases and reacting wall material. These calculations supply the wall mass flux (blowing rate) and wall-gas enthalpy tables needed to complete the analysis.

All of the above quantities are used to calculate the transient thermochemical response. For this analysis, the governing heat transfer equations are greatly simplified using Fick's law for binary diffusion. For the special case of unity Lewis number, the complete similarity between heat transfer and mass transfer is employed to solve the resulting equations. Finally, the mass addition of reacting wall material into the boundary layer modifies the heat transfer coefficient by the well-known "blocking effect"[2].

The five separate analysis modules are linked together by a labyrinth of files and require a considerable amount of manual input. The analysis codes include NOVA one-dimensional internal ballistics module, BLAKE nonideal gas thermochemical equilibrium module, TDK/MABL boundary layer properties module, TDK/ODE inert and reacting gas-wall properties chemistry module, and MACE thermal response and surface erosion module. The above procedure is complex, considerable manual input is required, and a time-dependent solution is a tedious procedure.

The equations that govern an ablation model for convective heat transfer and mass addition to a chemically reacting boundary layer are quite difficult to solve. Fortunately, a series of physical assumptions reduces the problem so meaningful results can be obtained, and include (1) one-dimensional steady-state ablation; (2) convective heat transfer based upon a constant steady-state value; (3) mass loss in the form of gas phase diffusion; (4) melt runoff where the melt layer is assumed to be infinitesimally thin; (5) complete species diffusion in the melt layer; (6) no species diffusion in the solid phase; (7) melt layer obeying a prescribed phase diagram for composition versus temperature; (8) diffusion-controlled combustion; (9) unity Lewis and Prandtl numbers; and (10) equilibrium chemistry[12].

Thermochemical ablation involves reacting flow, ablation products, diffusion, eddy turbulence, radiation, gas-wall reaction zone, heat transfer, mass transfer, temperature gradients, thermal stress cracking, microcrack erosion, surface melting layer, and mechanical removal. The ablation model employed in this analysis includes the gas, the solid wall, the melt layer, heat transfer by convection and radiation, surface temperature effects, mass transfer at the gas-wall interface, enthalpy at the gas-wall interface, and mechanical erosion. Ablation products include all material coming off the wall, in gas, solid, and liquid phases. Blowing is gas coming off the wall and diffusing into the boundary layer.

The two types of thermochemical ablation modeling available are the Navier-Stokes approach or the engineering approach. The Navier-Stokes model includes the futuristic approach, with the fully reacting gas Navier-Stokes equations coupled with surface chemistry and in-depth heating. The engineering model includes the practical approach, with decoupled fluid flow (boundary layer and inviscid core), interior ballistics, boundary layer heat transfer, and thermal response analysis. This analysis also assumes equilibrium chemistry for ablation, unity Lewis and Prandtl numbers, and similarity between heat and mass transfer.

Full Navier-Stokes modeling with chemistry requires few assumptions, is physically based, lacks micro-models for surface chemistry, lacks micro-models for turbulence, lacks micro-models for gas phase chemical kinetic mechanisms, and takes extensive computer resources.

Engineering approach modeling is relatively straightforward, whereby each mechanism's importance is identified, modest computer resources are needed, parametric analysis is possible, and incremental upgrades are feasible. However, this approach requires engineering judgment, and extrapolations may be questionable.

The engineering approach core assumptions include (1) test data support unity Lewis number (with similarity existing between heat and mass transfer); (2) the computed chemical ablation potential B_a

values, which can be calculated from equilibrium chemistry; (3) immediate molecule-wall reactions forming equilibrium products; (4) second-order importance of reacting chemistry on the blowing potential and heat transfer interaction; (5) the concept of a boundary layer; and (6) the concept of an inviscid core.

Following is the relationship between the various temperature scales[17]:

$$(F-32)/180 = C/100 = (K-273)/100 = (R-492)/180 \quad (1)$$

Figures 2 through 5 show NOVA travel and time versus pressure, velocity, temperature, and film coefficient data for the 155-mm M203 gun system for TDK/MABL input. It should be noted that at this stage of development, TDK/MABL will not take negative velocities and smoothing of the linkage files may be required. For the entire NOVA/BLAKE/ TDK/MACE analysis, all unknown parameters can be determined by experiment. Incidentally, NOVA-predicted energy loss order is highest for the gas, then for the projectile, and then for the tube.

Figure 6 plots BLAKE pressure-temperature-compressibility data for the 155-mm M203 gun system for TDK/MABL and TDK/ODE input. BLAKE thermochemical equilibrium products are confirmed by experimental Arrhenius testing, experimental combustion gas analysis, and past experimental data for combustion product species.

The TDK/MABL module uses a simple backwards-difference implicit integration method to calculate the flow variables, while the chemical relaxation equations are integrated using a first-order implicit integration method to insure numerical stability in near equilibrium flows. The code calculates flows with mass addition at the wall (blowing), transport properties, heat transfer, quasi-steady-state H_{gw}, and Mollier chart gas properties. Software and Engineering Associates modifications to TDK/MABL include real gas binary mixture chemistry, finite rate chemical kinetics, generalized chemical equilibrium, a fully implicit back-difference subroutine, and linkage files to MACE.

This code analyzes the propellant-wall boundary layer with a different secondary exhaust composition transpiring through the wall, and calculates the resultant boundary layer effect. The primary and secondary flows are treated as a binary mixture, where the rate of mixing is controlled by an eddy-viscosity model. Equilibrium, frozen chemistry at an initial equilibrium composition, or finite rate kinetics can be used to govern the flow chemistry. The boundary layer equations for compressible turbulent flow can be derived from the time-dependent Navier-Stokes equations using the Reynolds time-averaging procedure and the usual boundary layer order-of-magnitude assumptions. For this work, the simplified equilibrium chemistry was used although nonequilibrium chemistry (generalized finite rate chemical kinetics) is possible.

For TDK/MABL, the boundary layer equations are written in a curvilinear coordinate system in which s is the wetted length along the wall and y is measured normal to it (x is axial distance measured along the center line). It is assumed that the lateral and transverse curvature terms can be neglected, resulting in simplified conservation equations for continuity, momentum, and energy[26].

The TDK/MABL analysis is the weak link in the total erosion analysis, since it does not include time- dependent effects. The resulting 155-mm M203 gun system TDK/MABL output data is subsequently used for MACE code input. Figure 7 plots the TDK/MABL axial location-time-adiabatic wall enthalpy data. The recovery enthalpy at the adiabatic wall temperature (H_r) is the potential chemistry driver where the heat transfer approaches zero. Figure 8 plots the TDK/MABL axial location-time-adiabatic wall temperature data. This temperature (T_{aw}) is the potential temperature without reactions. Figure 9 plots the TDK/MABL axial location- time-cold wall heat transfer rate data. This heat flux (Q_{cw}) is the wall heat flux evaluated at the cold wall temperature. At present, TDK/MABL cannot tolerate unsmoothed negative velocities, negative pressure gradients, or recirculation. The plots of the TDK/MABL output indicate that the peak heat load was located approximately 1 to 2 feet from the breech. Therefore, the boundary layer parameters (recovery enthalpy and cold wall heat transfer rate) were extracted from the TDK/MABL output as a function of time at the 1- and 2-foot locations for MACE code input. The

TDK/MABL analysis shows that guns add only a small amount of mass to the boundary layer, which thickens it, and decreases heat transfer conduction to the wall.

The TDK/MABL heat and mass transfer model includes the following three equations: For mass addition to the boundary layer

$$r_e U_e Ch_o = Q_{cw}/(H_r - H_{gw}) \quad (2)$$

where r_e is edge density, U_e is edge velocity, Ch_o is Stanton number without blowing, Q_{cw} is cold wall heat transfer, H_r is recovery enthalpy, and H_{gw} is gas-wall enthalpy. For the heat-to-mass transfer ratio

$$r_e U_e Ch_b = Mdot_g/B_a; \; Le = 1 \quad (3)$$

where Ch_b is Stanton number with blowing, $Mdot_g$ is gas mass transfer, Le is the Lewis number, and B_a is ablation potential. For the overall correlation between these two equations

$$Ch_b/Ch_o = f(B_a, M_w) = 1 - (h \, Mdot_g/r_e U_e Ch_o) \quad (4)$$

where M_w is molecular weight, $h = a(M_{we}/M_{wi})^{**b}$, h is related to the molecular diffusion of the gas into the boundary layer, M_{we} is the molecular weight of the inviscid core at the edge of the boundary layer, M_{wi} is the molecular weight of the injected gas, a is the coefficient, and b is the exponent.

For a description of the TDK/ODE analysis, see Reference 17; also see Reference 33.

The following 155-mm M203 gun system TDK/ODE output data is for MACE code input. Figure 10 plots TDK/ODE pressure-temperature-inert H_{gw} data for chromium. Figure 11 plots TDK/ODE pressure- temperature-reacting wall H_{gw} data for chromium. Figure 12 plots TDK/ODE pressure-temperature-C_{cg} data (transposed) for chromium. Figure 13 plots TDK/ODE pressure-temperature-B_a data (transformed) for chromium. Figure 14 plots TDK/ODE pressure-temperature-inert H_{gw} data for gun steel. Figure 15 plots TDK/ODE pressure-temperature-reacting wall H_{gw} data for gun steel. Figure 16 plots TDK/ODE pressure-temperature-C_{cg} data (transposed) for gun steel. Figure 17 plots TDK/ODE pressure-temperature-B_a data (transformed) for gun steel. B_a is the thermochemical ablation potential.

Choosing chemical equilibrium species requires considerable experience, since many equilibrium species may not actually exist. Experimental data or a chemical kinetic analysis will determine if species should be omitted due to kinetic blocking.

The reaction-limiting temperature (T_{react}) is at the onset temperature of the exothermic reaction for a given pressure; while the diffusion-limiting temperature (T_{diff}) is at the diffusion-limited equilibrium temperature point of the exothermic reaction for a given pressure. The best way to determine T_{react} and T_{diff} is by an Arrhenius tester. The next best way is by a proposed time-dependent chemical kinetics code, but for the purpose of this work, this chromium and gun steel data are acquired from Figures 11 and 15, respectively. Figure 11 chromium data includes respective P(psi)-T_{react}(R)-T_{diff}(R) triplets of 10-1800- 2200, 100-2000-2400, 1000-2350-2800, 2500-2400-3000, 5000-2600-3000, 15000-2800-3200, and 30000-3000-3400. Figure 15 gun steel data includes respective P(psi)-T_{react}(R)-T_{diff}(R) triplets of 10-800-1600, 100-1150-2000, 1000-1200-2400, 2500-1350-2600, 5000-1400-2800, 15000-1550-3000, and 30000-1600-3000.

The TDK/ODE ablation model assumes that as the gas diffuses to the wall, it reacts to form equilibrium products as follows:

$$B_a = (C_w - C_{cg})/C_g = (C_{pg} - C_g)/C_g \quad (5)$$

where B_a is the ablation potential, C_w (constant) is the mass fraction of wall material, C_g (constant) is the mass fraction of the gas edge, C_{cg} is the mass fraction of condensed phase products (counted on the wall surface, not counted off the wall surface), and C_{pg} is the mass fraction of product gas.

Figure 12 shows C_{cg} (Cr(s) mass fraction) with respect to pressure and temperature. At gun pressures with a gas oxidizer-chromium fuel ratio (O/F) of 0.5, Cr(s) is in equilibrium with Cr_2O_3(s) from ambient temperature up to its metal melting

temperature (3800° to 4000°R). In Figure 12, C_{cg} (mass fraction of Cr(s) before reaction onset) equals 0.3373 at gun conditions. By definition, C_w is the percent fuel = 1.0/1.5 = 0.6667 and C_g is the percent gas = 1 - C_w = 0.3333. Figure 13 shows B_a as a function of gun pressure and temperature, where B_a = $(C_w - C_{cg})/C_g$ = 0.991 and is required for MACE input.

This chromium case was run for O/F = 0.1, C_w = 0.9091, C_g = 0.0909, C_{cg} = 0.819, and B_a = 0.991; and it shows that B_a is independent of gun pressures, independent of O/F, but very dependent on stoichiometry. B_a is fixed by chosen reactant and product stoichiometry. Both B_a and C_{cg} are chosen here where the metal(sol) starts to react, although experimental data would be a better approach. C_{cg} uses only the metal(sol) and not the metal(liq) or metal(gas).

Figure 16 shows C_{cg} for the gun steel(sol) mass fraction with respect to pressure and temperature. The computations show that C_{cg} for gun steel was nearly identical to C_{cg} for iron, probably due to the fact that iron comprises approximately 95 percent of gun steel. For the purposes of this paper, C_{cg} for iron is used to illustrate these results, although this same illustration is true for the other gun steel metals, which add only a very minor correction. At gun pressures with an O/F of 0.5, Fe(A) is in equilibrium with Fe_3O_4(s) from ambient to 1000°R, Fe(A) is in equilibrium with FeO(s) from 1000° to 2100°R, Fe(C) is in equilibrium with FeO(s) from 2100° to 2900°R, and Fe(D) is in equilibrium with FeO(L) from 2900° to its metal melting temperature (3200° to 3400° R). Fe(s) is a combination of Fe(A), Fe(C), and Fe(D). The literature[51] shows that the equilibrium of Fe(A) with Fe_3O_4(s) from ambient to 1000°R does not exist and that it is all Fe(A). Thus in Figure 16, C_{cg} which is the mass fraction of Fe(s) before reaction onset, equals 0.136 at gun conditions. Again, by definition, C_w is percent fuel = 1.0/1.5 = 0.6667, and C_g is percent gas = 1 - Cw = 0.3333. Figure 17 shows B_a as a function of gun pressure and temperature, where B_a = $(C_w - C_{cg})/C_g$ = 1.59 and is required for MACE input.

The iron case was run for O/F = 0.1, C_w = 0.9091, C_g = 0.0909, C_{cg} = 0.7646, and B_a = 1.59; and again it shows that B_a is independent of gun pressures, independent of O/F, but very dependent on stoichiometry. Again, the following is true: B_a is fixed by chosen reactant and product stoichiometry, both B_a and C_{cg} are chosen where metal(s) starts to react although experiment would be better, and C_{cg} uses only the metal(sol) and not the metal(liq) or metal(gas).

The TDK/ODE thermochemical equilibrium products are confirmed by experimental Arrhenius testing (thermal analysis), experimental combustion gas analysis for metal products (gas chromatography, mass spectrometry, x-ray diffraction), experimental surface analysis for metal products (Auger spectrometry, ESCA spectrometry) and past experimental data for combustion product species. Combustion gas analysis shows that metallic combustion products generally quench to the same metal products. This analysis calls on experience and is difficult to automate.

TDK/ODE may zero out the negative B_a values above the melt temperature of the wall material. Although this requires refinement, it does not affect this analysis since melted material is instantly removed, by definition.

It should be noted that the TDK/ODE thermochemical equilibrium calculations, which generated B_a and H_{gw} tables, included the effects of complex chemical reactions, vaporization, melting, and metal alloys.

TDK has three chemistry options. The TDK/ODE chemical equilibrium option is used for this work and predicts maximum recession. Therefore, this option is very useful from a gun design standpoint. The TDK/ODK finite rates chemical kinetics Arrhenius-type option predicts "actual" recession. Unfortunately, this option was not used for this analysis, because this module currently lacks sufficient input data for it to be a practical tool. The TDK/ODE frozen chemistry option predicts no recession, and was not used here except to show that erosion does have a chemical component.

In summary, the TDK/ODE chemical equilibrium option was chosen since it is a practical approximation of gun barrel interior ballistics chemistry, where sufficient activation energy coupled with lots of collisions generates fast reaction rates,

high temperature, and high pressure for the given time frame.

The MACE code solves the one-dimensional heat conduction equation, includes mechanisms that control internal decomposition, and uses an implicit Newton's method boundary condition with an explicit interior solution. Software and Engineering Associates enhancements include the surface recession boundary options determined by simple conduction, constant temperature sublimation, a Munson-Spindler-type relationship (Arrhenius-type, multiple equations, primary T, secondary P), a carbon-oxygen reaction, or a generalized chemistry boundary condition (diffusion-based, thermochemical ablation). In addition to the above boundary conditions, the surface material may be removed by mechanical erosion, including gas "flow," particulate "flow," droplet "flow," and boundary layer shear stress. Up to ten materials may be considered with heat capacities, with/without 100 percent contact, contact resistances, and radiation gaps at each interface. Heat blocking due to mass injection can be either linear or nonlinear. Convective heat transfer and boundary layer properties may be input directly or input through a linkage file with a heat transfer code. Heating rates may be modified by angle-of-attack, surface roughness, nonisothermal wall, or protuberance heating. Material properties may be constant or vary as a function of temperature. The variable material properties may be irreversible based on maximum temperature or reversible based on current temperature. The output is written to a file that may subsequently be used as input to a plot program, thermal stress program, or a vehicle mass loss and drag (aeroheating) program. The program uses either spherical, cylindrical, or rectangular specified coordinates[27].

The MACE code calculates the actual thermochemical erosion response. The inputs include thermal properties, Mollier table for inert wall, Mollier table for reacting wall, mass addition parameter tables, and boundary layer parameters.

The following 155-mm M203 gun system MACE output data predicts surface erosion, surface temperature, and temperature profiles for each axial location case. Figure 18 plots this MACE T_{react}-time-recession (S) data for chromium at station 1. Figure 19 plots this MACE T_{react}-time-recession rate (SDOT) data for chromium at station 1. Figure 20 plots this MACE T_{react}-time-cold wall heat transfer rate (Q_{cw}, cold wall heat flux) data for chromium at station 1. Figure 21 plots this MACE T_{react}-time-hot wall heat transfer rate (Q_{hw}, hot wall heat flux) data for chromium at station 1. Figure 22 plots this MACE T_{react}-time-wall temperature (T_{wall}) data for chromium at station 1. Figure 23 plots this MACE T_{react}-time-recession (S) data for chromium at station 2. Figure 24 plots this MACE T_{react}-time-recession rate (SDOT) data for chromium at station 2. Figure 25 plots this MACE T_{react}-time-cold wall heat transfer rate (Q_{cw}) data for chromium at station 2. Figure 26 plots this MACE T_{react}-time-hot wall heat transfer rate (Q_{hw}) data for chromium at station 2. Figure 27 plots this MACE T_{react}-time-wall temperature (T_{wall}) data for chromium at station 2.

Figure 28 plots this MACE T_{react}-time-recession (S) data for gun steel at station 1. Figure 29 plots this MACE T_{react}-time-recession rate (SDOT) data for gun steel at station 1. Figure 30 plots this MACE T_{react}-time-cold wall heat transfer rate (Q_{cw}) data for gun steel at station 1. Figure 31 plots this MACE T_{react}-time- hot wall heat transfer rate (Q_{hw}) data for gun steel at station 1. Figure 32 plots this MACE T_{react}-time-wall temperature (T_{wall}) data for gun steel at station 1. Figure 33 plots this MACE T_{react}-time-recession (S) data for gun steel at station 2. Figure 34 plots this MACE T_{react}-time-recession rate (SDOT) data for gun steel at station 2. Figure 35 plots this MACE T_{react}-time-cold wall heat transfer rate (Q_{cw}) data for gun steel at station 2. Figure 36 plots this MACE T_{react}-time-hot wall heat transfer rate (Q_{hw}) data for gun steel at station 2. Figure 37 plots this MACE T_{react}-time-wall temperature (T_{wall}) data for gun steel at station 2.

The A723 melting point is 1452°C or 3106°R, but 3258°R was used for MACE input as a better approximation of gun steel. The chromium melting point is 1845°C or 3813°R, but 3834°R was used for MACE input as a better approximation of the chromium plated surface. Density, conductivity, and specific heat data for MACE input are from the NOVA data base.

The MACE calculations used the TDK/ODE tables and the TDK/MABL boundary layer parameters for the boundary conditions. The purely equilibrium

results indicate that an enormous amount of wall metal reacts with the hot gases in the boundary layer. Because the preceding analysis was for equilibrium flow, it only represents a limiting case.

Since the chemical kinetics for the gas-wall interaction has not been studied to date, the temperatures where the kinetics begin and equilibrium is achieved are parametrically stacked for each case. This *f-function* data can be determined experimentally with standard test techniques. An important experimental test to determine T_{react}, T_{diff}, and the cubic Arrhenius *f-function* is by using a thermogravimetric analyzer (TGA) or differential scanning calorimeter (DSC)-type Arrhenius tester with captured combustion gases (or at least a pure gas of interest). Since reaction rate is a weak function of pressure, low pressure flow of propellant products or pure gas can be used in a TGA (dm versus T, up to 1000°C, cubic transition curve) or a DSC (dq versus T, up to 600°C, bell-shaped curve), since the extreme sensitivity of these instruments compensates for the much reduced pressure. Equilibrium data for iron suggests that T_{react} = 170°C and T_{diff} = 615°C. Equilibrium data for chromium suggests that T_{react} = 725°C and T_{diff} = 1390°C. The experimental Arrhenius method determines nonequilibrium (chemical kinetic) recession rates. The MACE code needs only the actual Arrhenius profile case for an "exact" solution.

It should be noted that an equilibrium analysis of iron and air at room temperature will show that the iron will combine with the oxygen to form iron oxides. Since common sense tells us that this reaction occurs over a time scale that is many orders-of-magnitude greater than the time scale of interest, it can be concluded that this system is not in equilibrium and therefore must be kinetically controlled. On the other hand, if the above system were evaluated at 5000°R (2504°C), the TDK/ODE calculations would be reasonable, and it could be concluded that the system would indeed be in equilibrium.

Although the temperatures and pressures associated with the gun barrel interior ballistics suggest the use of an equilibrium analysis, the transient thermal response of the wall requires a kinetic wall function relating the chemistry associated with the reacting wall and inert wall. At low temperatures the wall is inert, while at elevated temperatures the wall chemically reacts with the propellant. Therefore, it is assumed that there is a temperature below which no reactions occur, referred to as T_{react}. It is also assumed that there is another temperature above which the system is in complete equilibrium, referred to as T_{diff}. The above analysis requires many tedious steps, but the final answer is still not precisely known until an ancillary kinetic study is performed to determine T_{react} and T_{diff}.

As explained above, T_{react} and T_{diff} can be determined by an Arrhenius tester or by a proposed time- dependent chemical kinetics code. For the purpose of this work, the chromium and gun steel data used by TDK/ODE were obtained from Figures 11 and 15, respectively. The TDK/ODE Mollier table of $(H_{gw})_{react}$ (versus temperature and pressure) provides equilibrium values for T_{react} and T_{diff} for MACE input cases. T_{react} is at the onset temperature of the exothermic reaction and T_{diff} is at the diffusion-limited equilibrium temperature point of the exothermic reaction. These temperatures may be a weak function of pressure. Figure 11 chromium data includes respective P(psi)-T_{react}(R)-T_{diff}(R) triplets of 10-1800-2200, 100-2000-2400, 1000-2350-2800, 2500-2400-3000, 5000-2600-3000, 15000-2800-3200, and 30000-3000- 3400. Figure 15 gun steel data includes respective P(psi)-T_{react}(R)-T_{diff}(R) triplets of 10-800-1600, 100-1150-2000, 1000-1200-2400, 2500-1350-2600, 5000-1400-2800, 15000-1550-3000, and 30000-1600-3000.

For MACE analysis, radiation effects from emissivity and absorptivity are not a factor until about 4000°R. Using a past MACE code illustration, SEA has performed a considerable amount of analysis on reentry heating of graphite heat shields in air using carbon-air kinetic rate functions. Based on analysis and test data, it has been shown that below 1500°R the graphite does not react with the flow, and above 3000°R the system is in equilibrium, resulting in T_{react} = 1500°R and T_{diff} = 3000°R. Based on these results, the cubic transition function was formulated to relate the ratio of the kinetic reaction rate to the equilibrium rate when the surface temperature is between T_{react} and T_{diff}. The carbon-air kinetic rate function plots temperature (R) against mdot/$mdot_{diff}$ and begins at

1500°R as an exponential kinetic curve that is not diffusion-limited, and transitions to a diffusion-limited (equilibrium) curve at about 2700°R. Each chemical system requires additional analysis and possibly test data to determine the appropriate T_{react} and T_{diff}. Since these quantities are not known for the problem of interest, the MACE study performed a parametric analysis of T_{react} and T_{diff} using equilibrium enthalpies.

At this point in code development, single-shot comparisons of wall material erosion are preferable to absolute single-wall material calculations. For the given example, predicted single-shot thermochemical wall erosion is compared, where uncracked gun steel eroded by a factor of one hundred million more than uncracked chromium at the 1-foot axial position.

RECOMMENDATIONS

The proposed objective is to develop a unified modular thermochemical-mechanical design tool to model hot reacting gases under high pressure and high-speed flow and allow for continuous improvements.

Twenty years ago, the solid rocket propulsion community was faced with the same kind of module integration effort that the gun barrel erosion community faces today. Numerous programs were used to solve a portion of the overall problem, so that a composite solution could be produced. Disparities in solid rocket motor performance predictions prompted the development of a reference code, Solid rocket Performance Program (SPP)[26]. The SPP code incorporated many of the existing analysis tools of the time and, most important of all, embodied the community-accepted methodologies for the prediction of solid rocket performance. The SPP code combines six analysis modules, which are automatically linked together to allow the user to perform a complete analysis with a minimum of effort. Besides linking the modules together, the SPP code has a great deal of expertise incorporated in the analysis stream. Software and Engineering Associates are the authors of the SPP code and have a great deal of experience in linking separate analysis modules, which allow the user to easily solve a seemingly impossible problem. The thermochemical ablation and mechanical erosion analysis of gun barrels also requires a similar integration effort to solve these complex problems with minimal user interaction.

In the last twenty years, gun barrel technology has primarily focused on mechanical and metallurgical aspects with a secondary focus on erosion. Catastrophic gun barrel failures have been nearly eliminated, while thermochemical erosion (thermochemical ablation with mechanical erosion) problems have intensified due to performance requirements demanding the use of higher flame temperature propellants. Recently, due to Benet's interactions with the rocket community, an advanced thermochemical erosion computer model for gun barrels has been developed. Unfortunately, this erosion model has not been fully introduced to the gun community due to its many tedious steps and its lack of unification. At present, with this new erosion model, it takes a skilled analyst about two weeks to perform an erosion analysis on a new gun system. A detailed plan is recommended to further develop, unify, and simplify use of this thermochemical erosion method for the gun community.

Phase I efforts include the development of a unified program master control module with the existing interior ballistics, thermochemical equilibrium/kinetics, boundary layer, ablation, conduction, and erosion modules. The automated master control module would call each analysis module in the proper sequence, provide the appropriate linkages, and literally shorten the analysis time by a factor of ten.

Phase II efforts include the development of improved modules including a combined chemical equilibrium module, a generalized time-dependent chemical kinetics module to evaluate reaction rates at the wall, and mass transfer considerations that separate phase components. The level of effort associated with these three tasks is many times the Phase I effort.

Potential commercial market considerations include technology transfer to design new high performance gun systems for PM-TMAS, PM-ABRAMS, and PM-AFAS based on approximately thirty years experience designing

reentry vehicle nosetips and nozzles. This technology can also be used by the Department of Energy and the private power production industry to design improved erosion-resistant heat exchangers, pressure vessels, and piping for their typical high temperature pressurized reacting chemical flows.

U.S. Army operation and support cost reduction considerations include designing extended life gun barrels. For example, in high performance gun programs like PM-TMAS, PM-ABRAMS, and PM-AFAS that are pushing the materials technology limits, this technology can explain, design, and overcome thermochemical erosion-related barriers.

Regarding U.S. Army mission relevance, for five years the Army Armament Research, Development, and Engineering Center (ARDEC) has funded erosion modeling-related 6.2 programs in the areas of thermal management, advanced ammo and gun technology, thermal and erosion modeling, and high performance gun technology. These four programs have resulted in the Army's current gun erosion modeling code. In addition, ARDEC has funded similar programs for developed systems such as the 120-mm M256 annular erosion and M242 Bushmaster bore erosion problems, where significant insight was drawn from the same four 6.2 programs.

REFERENCES

1. von Karman, T., *Sorbonne Lectures*, 1951-1952; see also *Princeton University Lectures*, 1953; "Fundamental Approach to Laminar Flame Propagation," *AGARD Selected Combustion Problems*, Butterworths, London, 1954; and "Fundamental Equations in Aerothermochemistry," *Proc. 2nd AGARD Combust. Colloq.*, Liege, Belgium, 1955.
2. Reshotko, E., and Cohen, C.B., "Heat Transfer at the Stagnation Point of Blunt Bodies," NACA TN Number 3513, July 1955.
3. Cohen, C.B., Bromberg, R., and Lipkis, R.P., "Boundary Layers with Chemical Reactions Due to Mass Additions," Report No. GM-TR-268, The Ramo-Wooldridge Corporation, Los Angeles, CA, 1957.
4. Denison, M.R., and Dooley, D.A., "Combustion in the Laminar Boundary Layer of Chemically Active Sublimators," Publication No. C-110, Aeronutronic Systems, Inc., Glendale, CA, 1957.
5. Lees, L., "Convective Heat Transfer with Mass Addition and Chemical Reactions," *Combustion and Propulsion, Proc. 3rd AGARD Combust. Colloq.*, Palermo, Sicily, Pergamon Press, NY, 1958; see also *Recent Advances in Heat and Mass Transfer*, McGraw-Hill, New York, 1961.
6. *JANNAF Thermochemical Tables*, Thermal Research Laboratory, National Bureau of Standards, The Dow Chemical Co., Midland, MI, 1971.
7. Aerotherm Axi-Symmetric Transient Heating and Material Ablation Computer Program (ASTHMA 3), Acurex Corporation, Aerotherm Div., Mountain View, CA, 1972.
8. Conduction Ablation Reaction Erosion Program (CARE), TRW Defense and Space Systems Group, Redondo Beach, CA, 1973.
9. Passive Nosetip Technology Program (PANT I&II) for RV Erosion and Ablation: Erosion Shape Computer Code (EROS), ABRES Shape Change Code (ASCC), Updated ABRES Shape Change Code (ASCC 80), Maneuvering ABRES Shape Change Code (MASCC), Controlled Shaping for Ablation/Particle Erosion Code (COSHAPE), and Shape-Stable Nosetip Performance Prediction Code (ASCC85), Acurex Corporation, Aerotherm Div., Mountain View CA, 1974-1986.
10. Erosion Resistant Nosetip Technology Program (ERNT), TRW Defense and Space Systems Group, Redondo Beach CA, 1975.
11. Moody, H.L., Smith, D.H., Haddock, R.L., and Dunn, S.S., "Tungsten and Molybdenum Ablation Modeling for Reentry Applications," *Proc. 13th AIAA Aerospace Sciences Meeting*, Pasadena, CA, 20-22 January 1975.
12. Nickerson, Gary R., "A Steady State Model for the Thermochemical Ablation Performance of Binary Materials," Technical Memorandum #5003-00-01, Prototype Development Associates, Inc., Santa Ana, CA, 1975.
13. Nickerson, Gary R., "Erosion Resistant Materials for MaRV Application," Prototype Development Associates, Inc., Santa Ana, CA, 1976.
14. Reentry Vehicle Materials Technology Program (REVMAT), Prototype Development Associates, Inc., Santa Ana, CA, 1976.
15. Gomez, A.V., "Passive Transpiration Cooling Analysis (PCOOL-1D) for Chemically Reacting

Metallic Ablators," TRW Defense and Space Systems Group, Redondo Beach, CA, 1976.
16. Sherman, M.M., and Smith, D.H., "A Monte Carlo Statistical Uncertainty Analysis Method for Nosetip Recession Predictions," *Proc. 2nd AIAA/ASME Thermophysics and Heat Transfer Conference*, Palo Alto, CA, 24-26 May 1978; also Prototype Development Associates, Inc., Technical Memorandum, Santa Ana, CA, 1978.
17. Gordon, S., and McBride, B., "Computer Program for Calculation of Complex Chemical Equilibrium Compositions, Rocket Performance, Incident and Reflected Shocks, and Chapman-Jouguet Detonations (CET)," NASA SP-273, NASA Lewis Research Center, Cleveland, OH, 1971.
18. Levine, J., "Transpiration and Film Cooling Boundary Layer Computer Program (MABL)," *Finite Difference Computer Program for Solving Turbulent Boundary Layer Equations with Equilibrium Chemistry*, Volume I, N72-19312, 1971.
19. Murphy, A.J., Chu, E.K., and Kesselring, J.P., "AFRPL Graphite Performance Prediction Program," *Volume I: Recommendations for a Standardized Analytic Procedure for MX Missile Nozzle Throat Recession Calculations*, ADA016720, 1975; also Acurex Corporation, Aerotherm Div., Technical Memorandum, Mountain View, CA, 1975.
20. Coats, D.E., Levine, J.N., Nickerson, G.R., Tyson, T.J., Cohen, N.S., Harry, D.P., and Price, C.H., "A Computer Program for the Prediction of Solid Propellant Rocket Motor Performance," CPIA Publication 246, Ultrasystems, Inc., Irvine, CA, 1975.
21. Nickerson, G.R., Coats, D.E., and Hermsen, R.W., "A Computer Program for the Prediction of Solid Propellant (SPP) Rocket Motor Performance," Volumes I and III, Software and Engineering Associates, Inc., Santa Ana, CA, 1981.
22. Particle Impact Erosion Program (PIE) for Rocket Nozzle Recession Predictions: Chamber Flowfield Code (CFC) and Charring Material Ablation-Erosion Code (CMAE), Acurex Corporation, Aerotherm Div., Mountain View, CA, 1981-1983.
23. Moody, H.L., Haddock, R.L., and Miyazawa, E.T., "Rocket Nozzle Thermal Analysis Program: Rocket Nozzle Heating and Recession Code (ROHARE) and Rocket Nozzle Shape Change, Erosion and Conduction Code (ROSEC)," PDA Engineering, Santa Ana, CA, 1983.
24. Coats, D.E., Nickerson, G.R., Dang, A.L., Dunn, S.S., and Kehtarnavaz, H., "The Solid Propellant Rocket Motor Performance Computer Program (SPP)," Version 6.0, Software and Engineering Associates, Inc., Carson City, NV; also *Proc. 23rd AIAA/SAE/ASME Joint Propulsion Conference*, San Diego, CA, 1987.
25. Coats, D.E., Berker, D.R., and Dunn, S.S., "Boundary Layer Study: JANNAF Standard TDK/BLM Code; the Parabolized N/S Two-Phase Finite Rate Chemistry Code (VIPER); and the Modified Creare CFD Program (Fluent)," Software and Engineering Associates, Inc., Carson City, NV, 1990.
26. Nickerson, G., Berker, D., Coats, D., and Dunn, S., "Two-Dimensional Kinetics (TDK) Nozzle Performance Computer Program," by Software and Engineering Associates, Inc., Carson City, NV, for NASA Marshall Space Flight Center, Huntsville, AL, 1993.
27. Dunn, S.S., "Materials Ablation Conduction Erosion Program (MACE)," Software and Engineering Associates, Inc., Carson City, Nevada, 1989.
28. Dunn, S., and Sopok, S., Private Communications re: Joint Modification of the BLAKE, NOVA, TDK, and MACE Codes for Gun Barrel Erosion, Software and Engineering Associates, Inc., Carson City, NV, and U.S. Army ARDEC, Benet Laboratories, Watervliet, NY, 1992-1993.
29. Freedman E., "BLAKE - A Thermodynamic Code Based on Tiger: User's Guide and Manual," Technical Report #ARBRL-TR-02411, U.S. Army Ballistic Research Laboratory, Aberdeen Proving Ground, MD, 1982.
30. Gough, P., "The XNOVAKTC Code," Paul Gough Associates, NH, 1990.
31. BLAKE Code Modified for TDK/MACE Linkage, Software and Engineering Associates, Inc., Carson City, NV, and U.S. Army ARDEC, Benet Laboratories, Watervliet, NY, 1993.
32. NOVA Code Modified for TDK/MACE Linkage, Software and Engineering Associates, Inc., Carson City, NV, and U.S. Army ARDEC, Benet Laboratories, Watervliet, NY, 1993.
33. TDK/MACE Codes Modified for Gun Barrel Erosion, Software and Engineering Associates, Inc., Carson City, NV, 1993.
34. Nickerson G., Coats, D., and Dunn, S., "Material Ablation, Conduction, and Erosion (TDK/MACE) Analysis of Gun Systems," paper

presented at U.S. Army ARDEC, Benet Laboratories Research Seminar, Watervliet, NY, 1993.
35. 155-mm M203 Unicannon System Drawings, U.S. Army ARDEC, Dover, NJ, 1993.
36. Nickerson, G., Coats, D., and Dunn, S., "BLAKE/NOVA/TDK/MACE Code Short Course," Software and Engineering Associates, Inc., Carson City, NV, June 1994.
37. Garn, P., *Thermoanalytical Methods of Investigation*, Academic Press, NY, 1965.
38. Lodding, W., *Gas Effluent Analysis*, Marcel Dekker, NY, 1967.
39. Margrave, J., *The Characterization of High-Temperature Vapors*, John Wiley & Sons, NY, 1967.
40. Benson, S., *Thermochemical Kinetics - Methods for the Estimation of Thermochemical Data and Rate Parameters*, John Wiley & Sons, NY, 1968.
41. Fast, J., *Interaction of Metals and Gases*, Academic Press, NY, 1965.
42. Kofstad, P., *High-Temperature Oxidation of Metals*, John Wiley & Sons, NY, 1966.
43. Picard, J., Ahmad, I., and Bracuti, A., *Proceedings of the Tri-Service Gun Tube Wear and Erosion Symposiums*, U.S. Army ARDEC, Dover, NJ, 1970, 1972, 1977, and 1982.
44. Vassallo, F., and Brown, W., "Shock Tube Gun Melting Erosion Study," Calspan Corporation, Buffalo, NY, 1979.
45. Chufarov, G.I., et al., "Thermodynamics of the Oxidation of Metals," in *Surface Interactions Between Metals and Gases*, (V.I. Arkharov and K.M. Gorbunova, Eds.), Transl. by Consultants Bureau, NY, 1966.
46. Argent, B.B., and Birks, N., "Rate-Limiting Reactions in High Temperature Oxidation Processes," *High Temperature Materials - The Controlling Physical Processes*, Oliver & Boyd, Edinburgh and London, 1968.
47. Kamdar, M., Brassard, T., and Campbell, A., "A Metallographic Study of White Layers in Gun Steel," ARLCB-TR-78012, Benet Weapons Laboratory, Watervliet, NY, August 1978.
48. Morphy, C., and Fisher, E., "The Role of Carburization in Gun Barrel Erosion and Cracking," Calspan Corporation, Buffalo, NY, 1981.
49. Fisher, R., Szirmae, A., and Kamdar, M., "Metallographic Studies of Erosion and Thermo-chemical Cracking of Cannon Tubes," ARLCB-TR-83022, Benet Weapons Laboratory, Watervliet NY, May 1983.
50. Kamdar, M., and Venables, J., "Characterization of Bore Surface Layers in Gun Barrels," ARLCB-TR-84041, Benet Weapons Laboratory, Watervliet, NY, December 1984.
51. Alkidas, A., Morris, S., Christoe, C., Caveny, L., and Summerfield, M., "Erosive Effects of Various Pure and Combustion-Generated Gases on Metals - Part II," U.S. Army Materials and Mechanics Research Center, Watertown, MA, 1977; see also Part I, 1975.
52. Johnson, J., Caveny, L., and Summerfield, M., "Hot Gas Erosion of Gun Steel," U.S. Army Materials and Mechanics Research Center, Watertown, MA, 1979.
53. Krishnan, G., Scott, A., Wood, B., and Cubicciotti, D., "Effect of Transient Combustion Species on 4340 Steel," SRI International, Menlo Park, CA, 1979.
54. Fisher, E., and Morphy, C., "The Role of Oxygen in Gun Barrel Erosion and Cracking - A Shock Tube Gun Investigation," Calspan Corporation, Buffalo, NY, 1980.
55. Morphy, C., and Fisher, E., "Gas Chemistry Effects on Gun Barrel Erosion - A Shock Tube Gun Investigation," Calspan Corporation, Buffalo, NY, 1982.
56. Lin, S., "Auger Electron Spectroscopic Study of Gun Tube Erosion and Corrosion," *Applications of Surface Science*, Vol. 15, No. 1-4, 1983.
57. Lin, S., "Chemical Constituents of Eroded Gun Surfaces," *Applications of Surface Science*, Vol. 21, No. 1-4, 1985.

Fig 1 - Bore Erosion Analysis Procedure

NOVA / BLAKE

Temporal States: P, T

BL Edge Conditions: Pe(x,t), Ue(x,t), Te(x,t)

Compressibility Tables: Z(P,T)

TDK / MABL

BL Characteristics: Hr(T), Qcw(T)

TDK / ODE

Gas Properties: Ho(P,T)

Blowing Parameter: Bh(P,T)

Reacting Wall Gas Properties: H(P,T)

MACE

Surface Erosion

Surface Temperature

Temperature Profile

Fig 2 - Nova Pressure Data

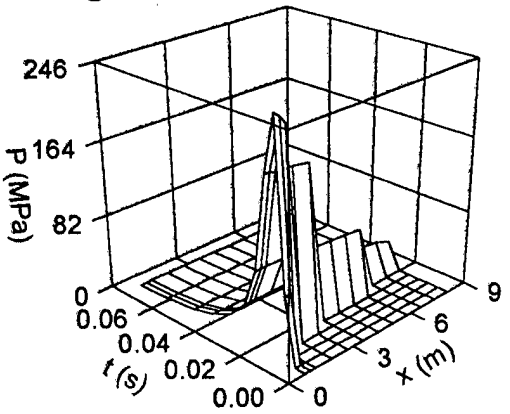

Fig 3 - Nova Vgas Data

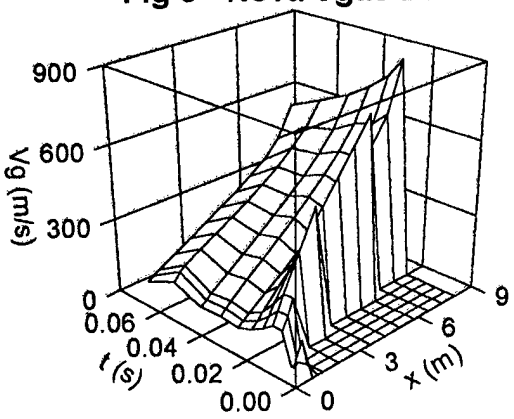

Fig 4 - Nova Tgas Data

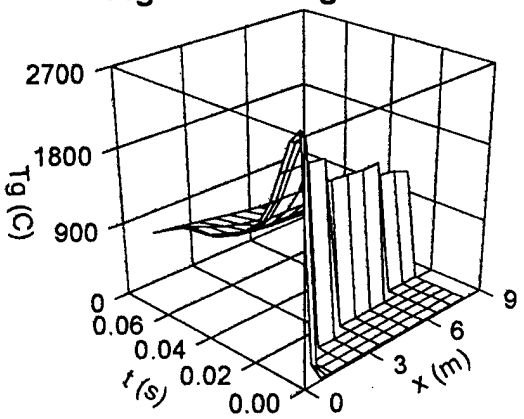

Fig 5 - Nova Hfilm Data

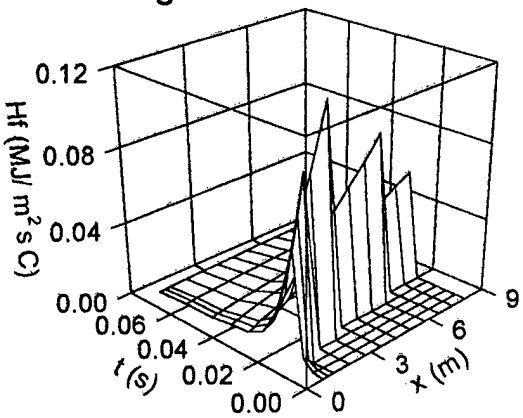

Fig 6 - Blake Compressibility Data

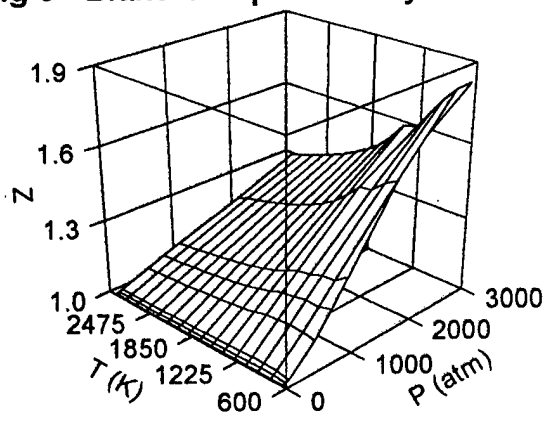

Fig 7 - TDK/MABL Hwall Data

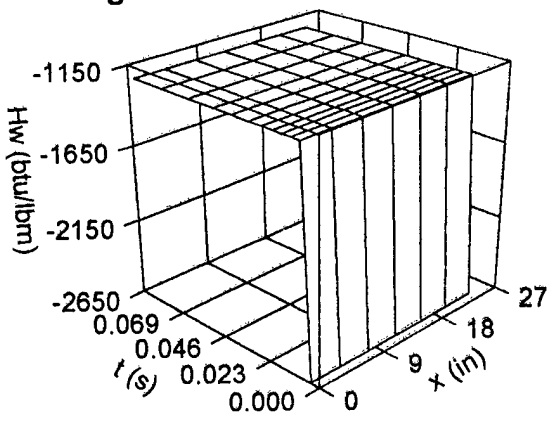

Fig 8 - TDK/MABL Twall Data

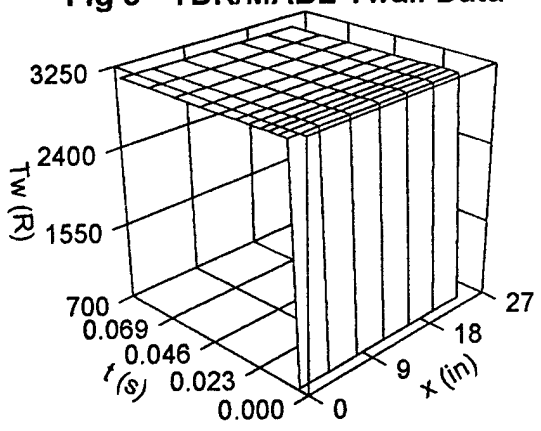

Fig 9 - TDK/MABL Qdot Data

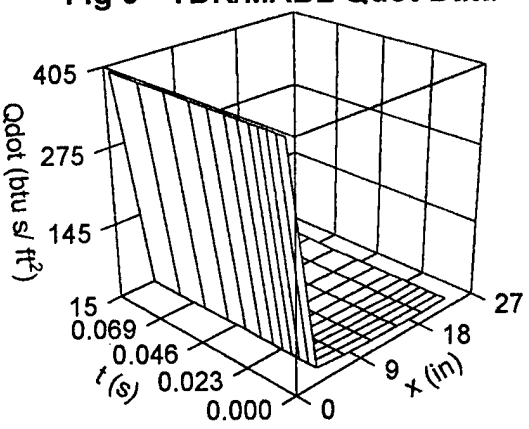

Fig 10 - TDK/ODE Hwgas$_{inert}$ Data

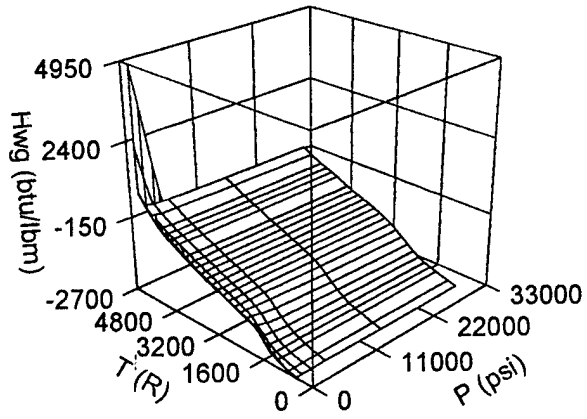

Fig 11 - TDK/ODE Hwgas$_{Cr,react}$ Data

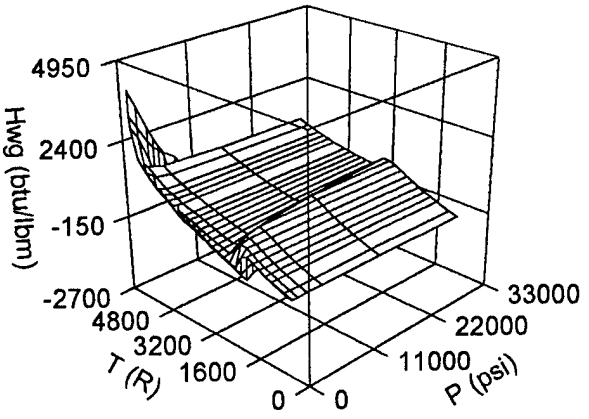

Fig 12 - TDK/ODE Ccg$_{Cr}$ Data

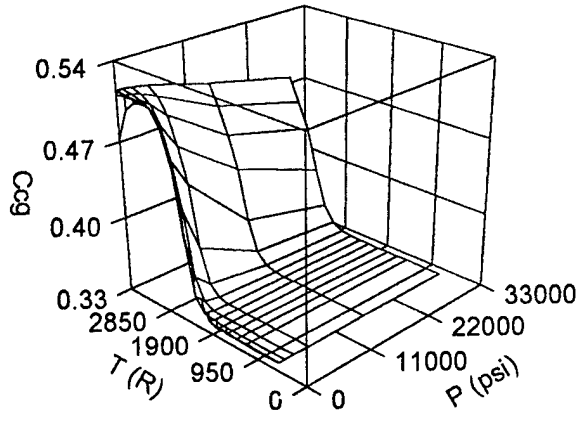

Fig 13 - TDK/ODE Ba$_{Cr}$ Data

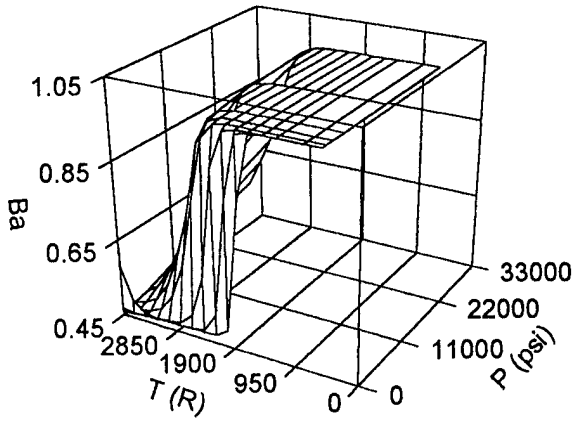

Fig 14 - TDK/ODE $Hwgas_{inert}$ Data

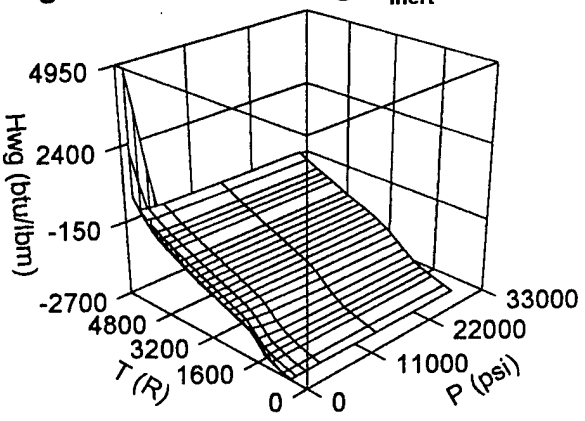

Fig 15 - TDK/ODE $Hwgas_{GS,react}$ Data

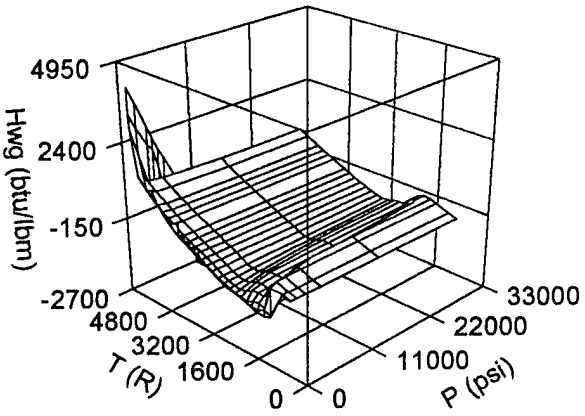

Fig 16 - TDK/ODE Ccg_{GS} Data

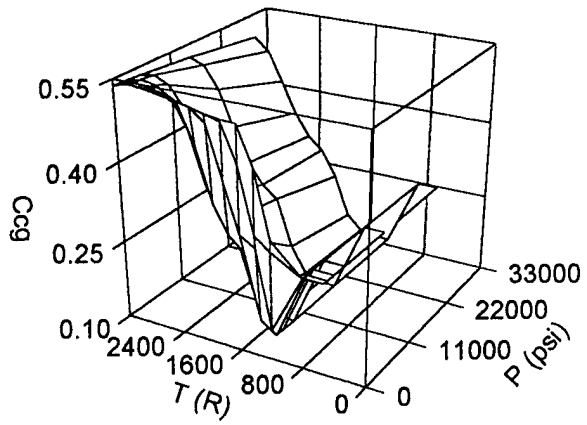

Fig 17 - TDK/ODE Ba_{GS} Data

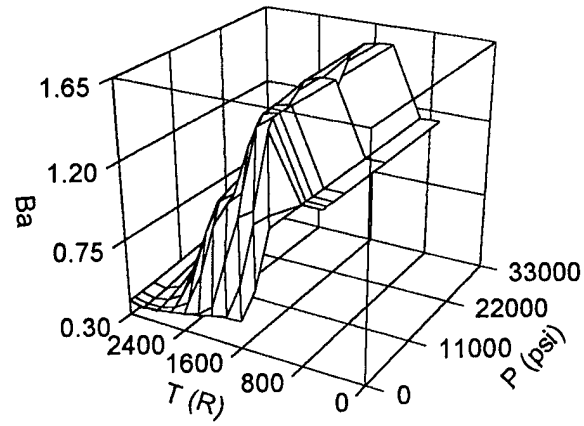

Fig 18 - MACE $S_{Cr,s1}$ Data

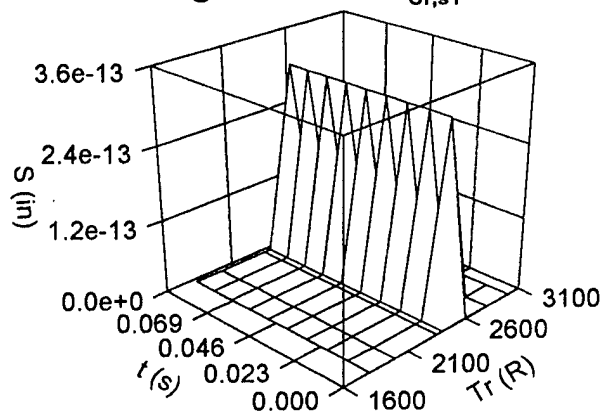

Fig 19 - MACE $Sdot_{Cr,s1}$ Data

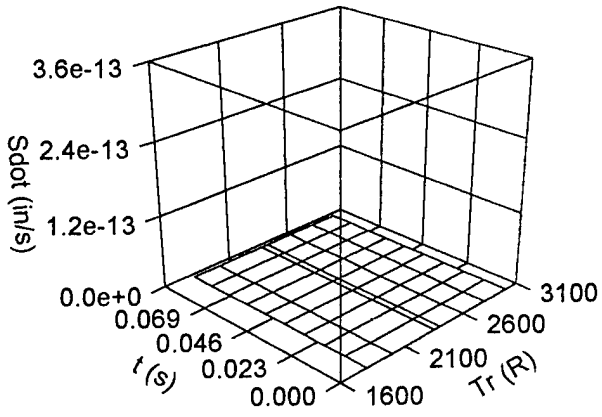

Fig 20 - MACE $Qdot_{cw,Cr,s1}$ Data

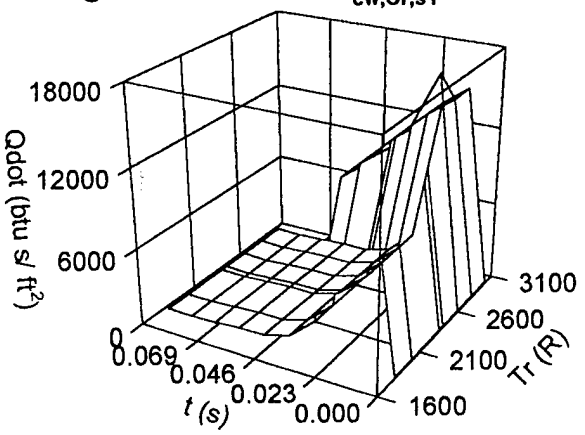

Fig 21 - MACE $Qdot_{hw,Cr,s1}$ Data

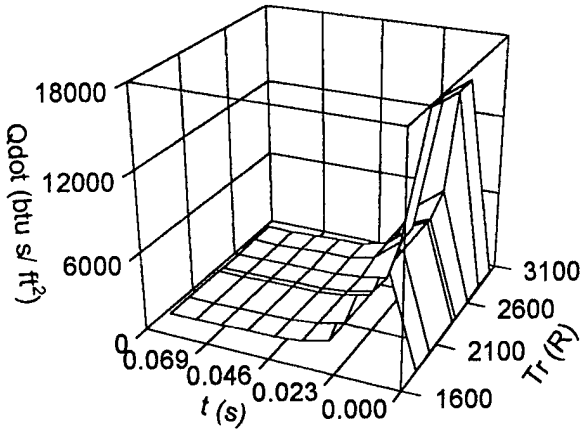

Fig 22 - MACE $Twall_{Cr,s1}$ Data

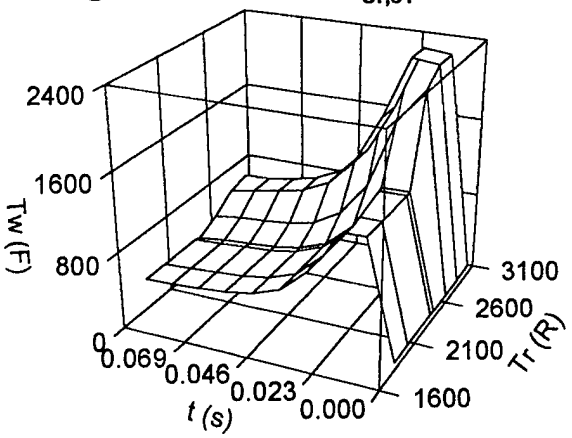

Fig 23 - MACE $S_{Cr,s2}$ Data

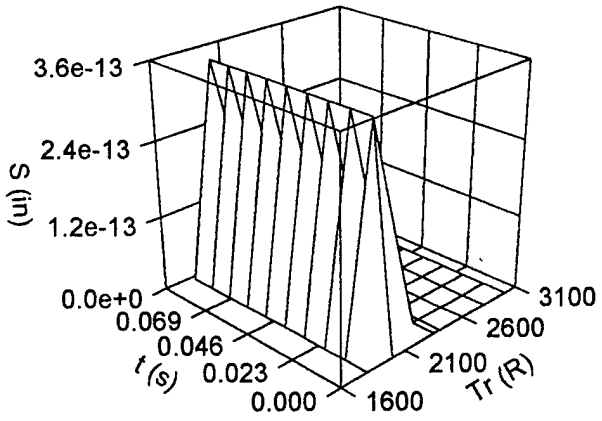

Fig 24 - MACE $Sdot_{Cr,s2}$ Data

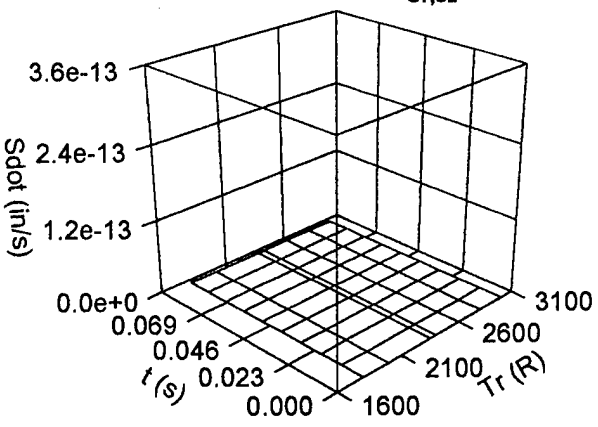

Fig 25 - MACE $Qdot_{cw,Cr,s2}$ Data

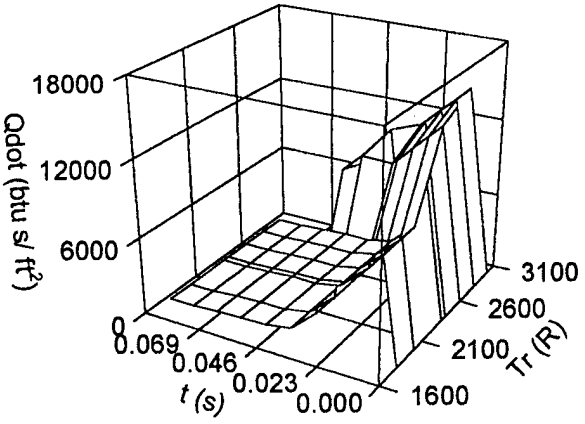

Fig 26 - MACE $Qdot_{hw,Cr,s2}$ Data

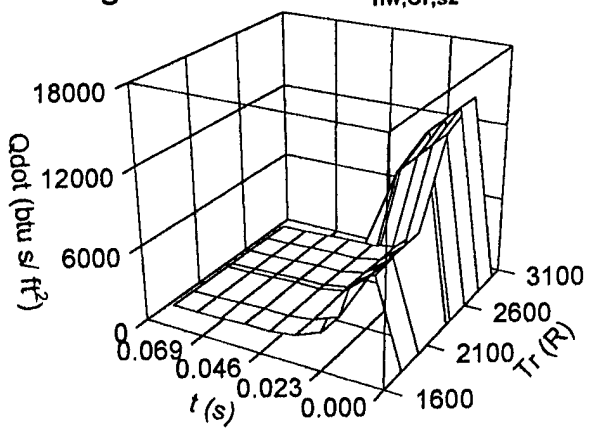

Fig 27 - MACE $Twall_{Cr,s2}$ Data

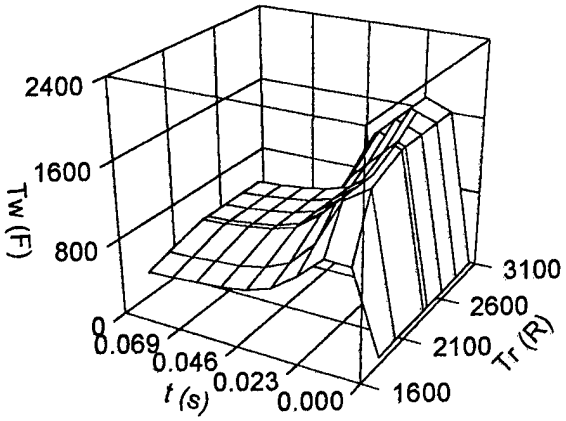

Fig 28 - MACE $S_{GS,s1}$ Data

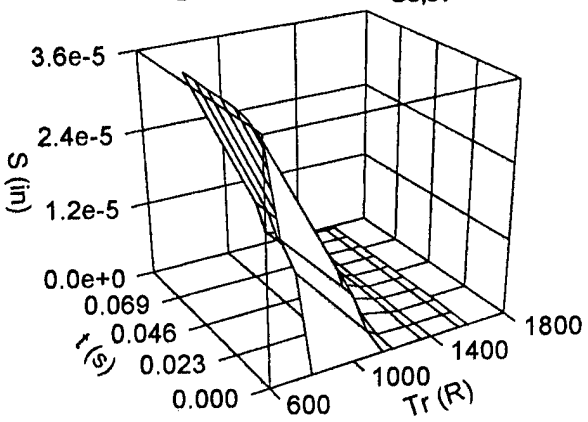

Fig 29 - MACE $Sdot_{GS,s1}$ Data

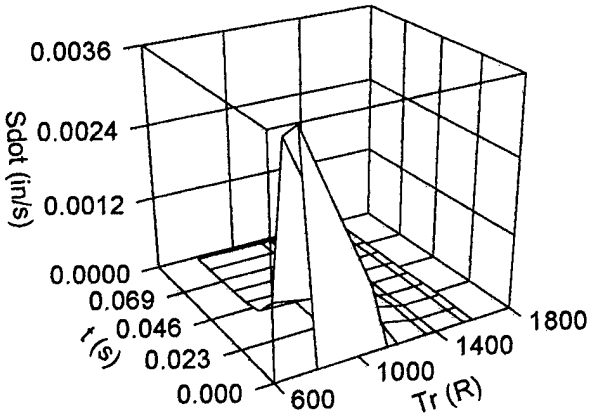

Fig 30 - MACE $Qdot_{cw,GS,s1}$ Data

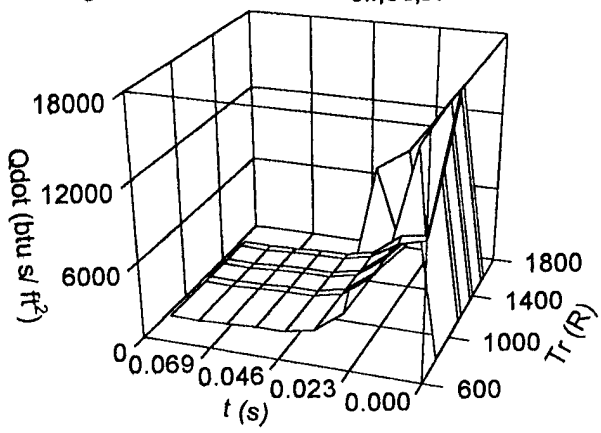

Fig 31 - MACE $Qdot_{hw,GS,s1}$ Data

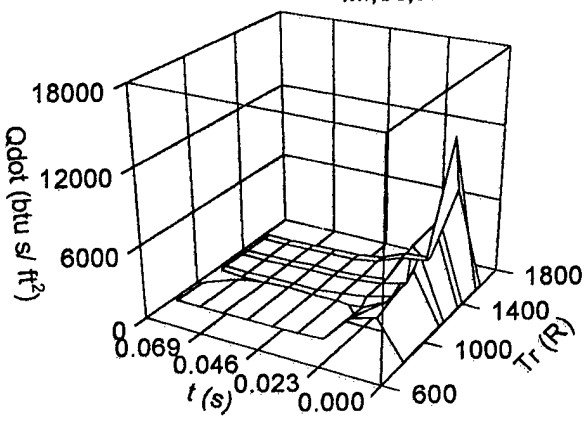

Fig 32 - MACE $Twall_{GS,s1}$ Data

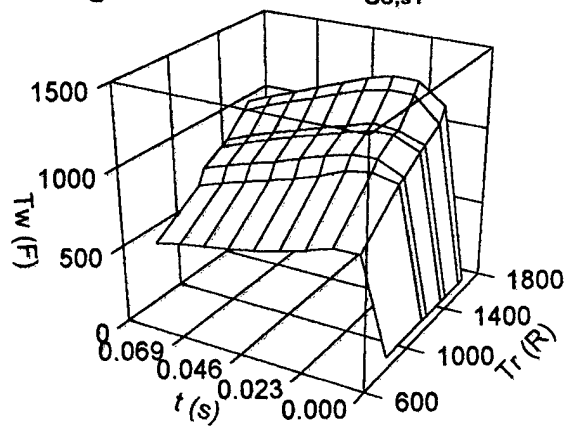

Fig 33 - MACE $S_{GS,s2}$ Data

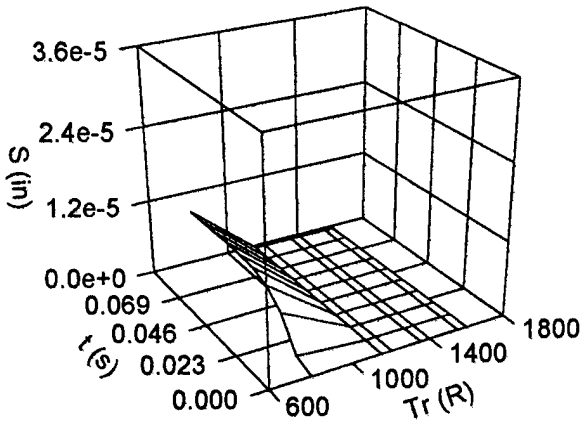

Fig 34 - MACE $Sdot_{GS,s2}$ Data

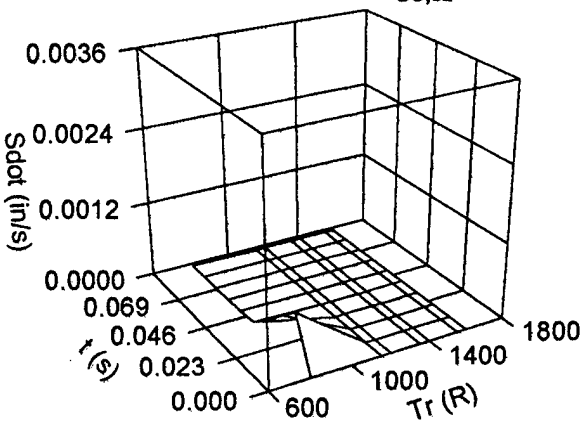

Fig 35 - MACE $Qdot_{cw,GS,s2}$ Data

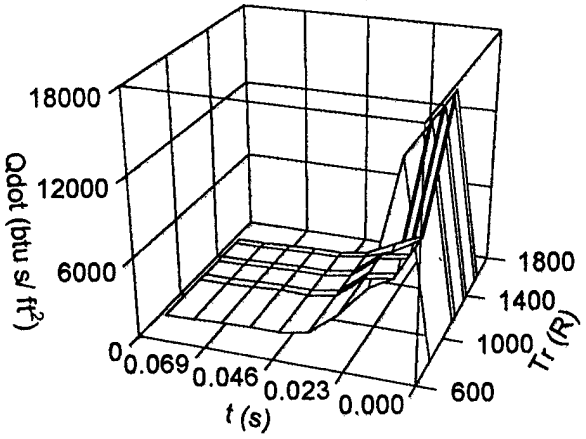

Fig 36 - MACE $Qdot_{hw,GS,s2}$ Data

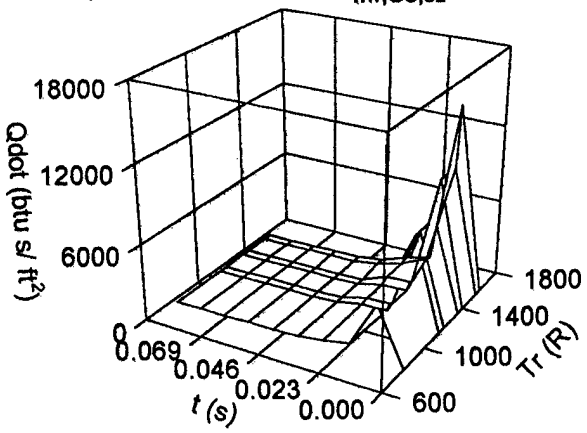

Fig 37 - MACE $Twall_{GS,s2}$ Data

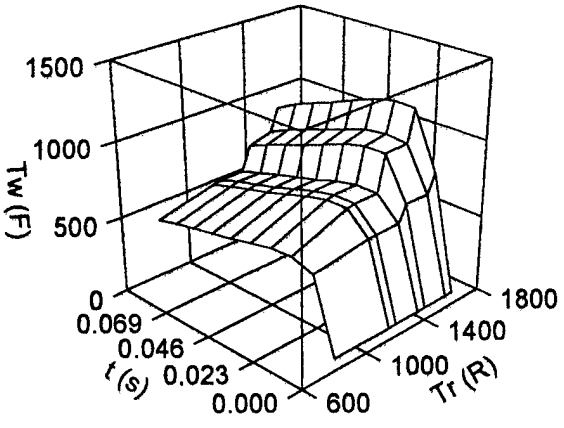

APPENDIX

NOVA 155MM M203 INPUT FILE EXAMPLE

```
M203 in 1400 in3 chamber from ARL
TFFFTTF00100000101000001000000000
   7599999    099999    0    0 2.000E-03
 1.000E+00 2.754E+02 1.000E-04 1.900E+00 5.000E-02 3.600E-03 2.000E-04 0.000E+00
    9    8    5    7    0    0    1    2    0    0    0    0    0    0    0    0
    0    0    2
 5.300E+02 1.470E+01 2.900E+01 1.400E+00
 5.300E+02 0.000E+00 0.000E+00 0.000E+00 0.000E+00 0.000E+00 0.000E+00
M30A1,RAD-E-069805   2.900E+00 4.217E+01 2.615E+01 5.720E-02 0.000E+00 0.000E+00
    7 4.173E-01 3.380E-02 9.481E-01 7.000E+00 0.000E+00    0 0.000E+00
 1.740E+04 4.243E-01 5.000E+04 0.000E+00 0.000E+00
 1.000E+04 6.918E-03 6.337E-01 6.000E+04 1.700E-03 7.864E-01 0.000E+00 8.100E+02
 2.770E-02 1.345E-04 6.000E-01
 1.760E+07 2.336E+01 1.243E+00 2.850E+01
 6.303E+06 3.613E+01 1.250E+00 1.538E+01
 0.000E+00 1.000E-02 1.100E-02 4.900E-02 5.000E-02 6.000E-02 6.100E-02 1.000E-01
 2.900E+00 3.900E+00 3.910E+00 3.290E+01 3.390E+01
 6.000E+00 6.000E+00 0.000E+00 0.000E+00 0.000E+00
 6.000E+00 6.000E+00 0.000E+00 0.000E+00 0.000E+00
 0.000E+00 0.000E+00 0.000E+00 0.000E+00 0.000E+00
 0.000E+00 0.000E+00 0.000E+00 0.000E+00 0.000E+00
 0.000E+00 1.000E+00 1.000E+00 1.000E+00 0.000E+00
 0.000E+00 1.000E+00 1.000E+00 1.000E+00 0.000E+00
 0.000E+00 0.000E+00 0.000E+00 0.000E+00 0.000E+00
 0.000E+00 0.000E+00 0.000E+00 0.000E+00 0.000E+00
 0.000E+00 3.690E+00 1.417E+00 3.336E+00 4.140E+00 3.336E+00 4.210E+00 3.371E+00
 1.717E+01 3.371E+00 3.126E+01 3.232E+00 4.607E+01 3.165E+00 4.786E+01 3.080E+00
 3.187E+02 3.080E+00
 0.000E+00 2.500E+02 4.000E-01 3.350E+03 1.000E+00 5.000E+03 1.550E+00 3.625E+03
 2.050E+00 3.250E+03 4.500E+00 2.500E+03 2.720E+02 1.500E+03
 7.770E+00 2.280E-01 7.000E-01
 4.327E+01 9.600E+01 1.400E+01 8.270E+00 4.327E+01 0.000E+00
 2.900E+00 3.000E+01 0.000E+00    3    0
 1.417E+00 1.000E+00 0.000E+00    1    2
 0.000E+00 0.000E+00 1.000E+00 1.000E+06
```

BLAKE 155MM M203 INPUT FILE EXAMPLE

```
CMT RUN AN ISOLINE FOR M30A1 PROPELLANT
CMT
FORMULA, KCRY, -795E3, K, 3, AL, 1, F, 6
TIT,  M30A1 PROPELLANT ...  T Calculations for P=3000
DES
REJ, O2, C(S)
REJ, C2N, C2H, C2, CH2O, NO2, H2S, S2O, SO2, K$, KOH$, K2O,
REJ, K2O2, KO2, HNO3, C, CH, K2, N,
REJ, KCO$, KSO$, K2O$, NA2$
REJ, C2H4, C2N2, C2H2, CH2
REJ, HNO, HNO3
REJ,K2S$
ORD,N2,CO,H2O,KOH,HS
RET
CM2, NC1260, 27.90, NG, 22.42, NQ, 46.84, EC, 1.49,
   KS, 1.0, ALC, .25, C, .1
ISOline, P, 3000, T, 3010.,15, 650.
TIT,  M30A1 PROPELLANT ...  T Calculations for P=2000
RET
ISOline, P, 2000, T, 3010.,15, 650.
TIT,  M30A1 PROPELLANT ...  T Calculations for P=1000
RET
ISOline, P, 1000, T, 3010.,15, 650.
TIT,  M30A1 PROPELLANT ...  T Calculations for P=750
RET
ISOline, P, 750, T, 3010.,15, 650.
TIT,  M30A1 PROPELLANT ...  T Calculations for P=500
RET
ISOline, P, 500, T, 3010.,15, 650.
TIT,  M30A1 PROPELLANT ...  T Calculations for P=100
RET
ISOline, P, 100, T, 3010.,15, 650.
TIT,  M30A1 PROPELLANT ...  T Calculations for P=50
RET
ISOline, P, 50, T, 3010.,15, 650.
TIT,  M30A1 PROPELLANT ...  T Calculations for P=10
RET
ISOline, P, 10, T, 3010.,15, 650.
TIT,  M30A1 PROPELLANT ...  T Calculations for P=5
RET
ISOline, P, 5, T, 3010.,15, 650.
STOP
```

TDK/MABL 155MM M203 INPUT FILE EXAMPLE

```
TITL  NOVA data file NOVA_DAT.01 for time =   0.004000
 EDG   1.000000E+01  0.000000E+00  4.117817E+02  7.224005E+02  4.100942E+01    1
 EDG   1.224634E-01
 EDG   1.000000E+01  2.900141E+01  4.158996E+02  7.152480E+02  4.060339E+01    2
 EDG   1.224634E-01
 EDG   1.000000E+01  3.900190E+01  6.184357E+01  5.880222E+02  2.202402E+01    3
 EDG   8.079854E-02
 TDK   1.000000E+00
END
*******************************************************************************
*Case 1: TITLE MABLE RUN FROM NOVA DATA ... TIME = .0040  ADIABATIC WALL
*Case 2: TITLE MABLE RUN FROM NOVA DATA ... TIME = .0040  COLD WALL
*******************************************************************************
DATA
 $DATA
 ODE= 1, ODK = 0, TDE = 1, NOVA = T,
 MABL = 1, IMABL = 0, MABLE = T,
 NOVAIN = 'NOVA_DAT.01',
 THERMO = '..\THERMO.DAT',
*******************************************************************************
*Case 1: BLANK
*Case 2: IRSTRT = 2,
*******************************************************************************
 $END
REACTANTS
C       6.H  7.549 O 9.901  N 2.451              27.90 -1.6916E8S  298.15F
C       1.                                          .1       0.0S  298.15F
C       3.H       5.O       9.N       3.          22.42   -88600.L  298.15F
C       1.H       4.O       2.N       4.          46.84   -22100.S  298.15F
C      17.H      20.O       1.N       2.           1.49   -25100.S  298.15F
K       2.S       1.O       4.                       1. -3.4266E5S  298.15F
C       2.H       6.O       1.                     .25  -6.642E4S  298.15F
OMIT            C                 CH              CH2               CH2O
OMIT            C2                C2H             C2H2              C2H4
OMIT            C2N               C2N2            HNO               HNO3
OMIT            H2S               K2              NO2               O2
OMIT            SO2               S2O             C(GR)             K(S)
OMIT            K(L)              KOH(A)          KOH(B)            KOH(L)
OMIT            K2O(S)            K2S(1)          K2S(2)            K2S(3)
OMIT            K2S(L)            N               H2SO4(L)          K2CO3(L)
OMIT            S(S)              K(S)            KOH(B)            K2O(S)
OMIT            K2S(L)            S(L)            H2O(L)            H2O(S)
OMIT            C(GR)
NAMELISTS
 $ODE
 PSIA =  T,
 RKT = T,
 OF = T,
 P =  41.0,
 T = 722,
 OFSKED = 100,
 BLAKE = T,
 PBLAKE=     5.000,    10.000,    50.000,   100.000,   500.000,   750.000,
          1000.000,  2000.000,  3000.000,
 TBLAKE=   650.000,   807.000,   965.000,  1122.000,  1279.000,  1437.000,
          1594.000,  1751.000,  1909.000,  2066.000,  2223.000,  2381.000,
          2538.000,  2695.000,  2853.000,  3010.000,
  COMP(1,1)= 1.00044E+00, 1.00110E+00, 1.00126E+00, 1.00118E+00, 1.00108E+00,
             1.00100E+00, 1.00092E+00, 1.00086E+00, 1.00080E+00, 1.00075E+00,
             1.00070E+00, 1.00066E+00, 1.00062E+00, 1.00059E+00, 1.00056E+00,
             1.00054E+00,
```

```
 COMP(1,2)= 1.00084E+00, 1.00213E+00, 1.00248E+00, 1.00236E+00, 1.00217E+00,
            1.00200E+00, 1.00185E+00, 1.00171E+00, 1.00160E+00, 1.00149E+00,
            1.00140E+00, 1.00132E+00, 1.00124E+00, 1.00118E+00, 1.00112E+00,
            1.00107E+00,
 COMP(1,3)= 1.00439E+00, 1.01008E+00, 1.01187E+00, 1.01175E+00, 1.01084E+00,
            1.00998E+00, 1.00923E+00, 1.00856E+00, 1.00797E+00, 1.00745E+00,
            1.00699E+00, 1.00657E+00, 1.00620E+00, 1.00587E+00, 1.00557E+00,
            1.00530E+00,
 COMP(1,4)= 1.00984E+00, 1.02035E+00, 1.02353E+00, 1.02350E+00, 1.02171E+00,
            1.01995E+00, 1.01844E+00, 1.01710E+00, 1.01592E+00, 1.01488E+00,
            1.01396E+00, 1.01313E+00, 1.01239E+00, 1.01172E+00, 1.01112E+00,
            1.01055E+00,
 COMP(1,5)= 1.08847E+00, 1.11650E+00, 1.12139E+00, 1.11585E+00, 1.11056E+00,
            1.09975E+00, 1.09140E+00, 1.08463E+00, 1.07878E+00, 1.07361E+00,
            1.06904E+00, 1.06497E+00, 1.06131E+00, 1.05801E+00, 1.05502E+00,
            1.05159E+00,
 COMP(1,6)= 1.15668E+00, 1.18397E+00, 1.18506E+00, 1.17411E+00, 1.16747E+00,
            1.14972E+00, 1.13635E+00, 1.12597E+00, 1.11726E+00, 1.10958E+00,
            1.10279E+00, 1.09674E+00, 1.09133E+00, 1.08643E+00, 1.08199E+00,
            1.07647E+00,
 COMP(1,7)= 1.23084E+00, 1.25337E+00, 1.24902E+00, 1.23201E+00, 1.22470E+00,
            1.19962E+00, 1.18079E+00, 1.16663E+00, 1.15508E+00, 1.14492E+00,
            1.13598E+00, 1.12801E+00, 1.12088E+00, 1.11443E+00, 1.10858E+00,
            1.10325E+00,
 COMP(1,8)= 1.53474E+00, 1.52744E+00, 1.49709E+00, 1.45511E+00, 1.44905E+00,
            1.39544E+00, 1.35356E+00, 1.32290E+00, 1.29944E+00, 1.28017E+00,
            1.26313E+00, 1.24803E+00, 1.23450E+00, 1.22231E+00, 1.21122E+00,
            1.19328E+00,
 COMP(1,9)= 1.82195E+00, 1.78308E+00, 1.72700E+00, 1.66232E+00, 1.59409E+00,
            1.58172E+00, 1.51821E+00, 1.47049E+00, 1.43481E+00, 1.40660E+00,
            1.38213E+00, 1.36062E+00, 1.34135E+00, 1.32394E+00, 1.30817E+00,
            1.29372E+00,
 NPBLAKE =     9, NTBLAKE =    16,
 $END
 $MABL
*******************************************************************************
*Case 1: ADBATC = 1,
*Case 2: ADBATC = 0,
*        XTQW = -1E6,146, TQW = 2*540., NTQW = 2,
*******************************************************************************
 NLPRNT = 250,
 DXI = .01, DXLIM = .05,1., NDXI = 50,
 $END
```

TDK/ODE 155MM M203 INPUT FILE EXAMPLE

```
*****************************************************************************
*Cases 1&2: TITLE T-P CALCULATION, 155 MM GUN, M30A1 PROPELLENT, NO METAL
*Cases 3&4: TITLE T-P CALCULATION, 155 MM GUN, M30A1 PROPELLENT, WITH CHROME
*Cases 5&6: TITLE T-P CALCULATION, 155 MM GUN, M30A1 PROPELLENT, WITH GUNSTEEL
*Cases 7&8: TITLE T-P CALCULATION, 155 MM GUN, M30A1 PROPELLENT, WITH IRON
*****************************************************************************
DATA
 $DATA
 ODE=           1
 THERMO = '..\THERMO.DAT',
 $END
REACTANTS
*****************************************************************************
*Cases 1&2:
*BLANK
*Cases 3&4:
*CR1.                                          100.          S         F
*Cases 5&6:
*FE1.                                           94.44        S         F
*NI1.                                            2.75        S         F
*CR1.                                            1.00        S         F
*MN1.                                            0.60        S         F
*MO1.                                            0.50        S         F
*C 1.                                            0.34        S         F
*SI1.                                            0.23        S         F
*V 1.                                            0.10        S         F
*P 1.                                            0.01        S         F
*S 1.                                            0.01        S         F
*AL1.                                            0.01        S         F
*TI1.                                            0.01        S         F
*Cases 7&8:
*FE1.                                          100.          S         F
*****************************************************************************
C      6.H  7.549 O 9.901  N 2.451             28.90 -1.6916E8S  298.15O
C      1.                                        .1       0.0S  298.15O
C      3.H      5.O      9.N      3.            22.42   -88600.L  298.15O
C      1.H      4.O      2.N      4.            46.84   -22100.S  298.15O
C     17.H     20.O      1.N      2.             1.49   -25100.S  298.15O
C      2.H      6.O      1.                      .25  -6.642E4S  298.15O
*****************************************************************************
*Cases 1,3,5,&7: NO OMITTED PRODUCTS
*Cases 2: OMIT C(GR), H2O(L)
*Cases 4: OMIT C(GR), CR2N(S), CRN(S)
*Cases 6: OMIT C(GR)
*Cases 8: OMIT C(GR)
*****************************************************************************
NAMELISTS
 $ODE
 PSIA =  T,
 TP = T,
 OF = T,
 P =  1,10,100,1000,2500,5000,15000,30000
 T = 6100,5800,5400,5200,5000,4800,
     4400,4200,4000,3800,3600,3400,
     3200,3000,2800,2600,2400,2200,
     2000,1800,1600,1400,1200, 800,
      540,
 OFSKED = 0.5,
 TABGEN = T,
 BLAKE = T,
 PBLAKE=     5.000,    10.000,    50.000,   100.000,   500.000,   750.000,
          1000.000,  2000.000,  3000.000,
```

```
TBLAKE=   650.000,   807.000,   965.000,  1122.000,  1279.000,  1437.000,
         1594.000,  1751.000,  1909.000,  2066.000,  2223.000,  2381.000,
         2538.000,  2695.000,  2853.000,  3010.000,

 COMP(1,1)= 1.00044E+00, 1.00110E+00, 1.00126E+00, 1.00118E+00, 1.00108E+00,
            1.00100E+00, 1.00092E+00, 1.00086E+00, 1.00080E+00, 1.00075E+00,
            1.00070E+00, 1.00066E+00, 1.00062E+00, 1.00059E+00, 1.00056E+00,
            1.00054E+00,
 COMP(1,2)= 1.00084E+00, 1.00213E+00, 1.00248E+00, 1.00236E+00, 1.00217E+00,
            1.00200E+00, 1.00185E+00, 1.00171E+00, 1.00160E+00, 1.00149E+00,
            1.00140E+00, 1.00132E+00, 1.00124E+00, 1.00118E+00, 1.00112E+00,
            1.00107E+00,
 COMP(1,3)= 1.00439E+00, 1.01008E+00, 1.01187E+00, 1.01175E+00, 1.01084E+00,
            1.00998E+00, 1.00923E+00, 1.00856E+00, 1.00797E+00, 1.00745E+00,
            1.00699E+00, 1.00657E+00, 1.00620E+00, 1.00587E+00, 1.00557E+00,
            1.00530E+00,
 COMP(1,4)= 1.00984E+00, 1.02035E+00, 1.02353E+00, 1.02350E+00, 1.02171E+00,
            1.01995E+00, 1.01844E+00, 1.01710E+00, 1.01592E+00, 1.01488E+00,
            1.01396E+00, 1.01313E+00, 1.01239E+00, 1.01172E+00, 1.01112E+00,
            1.01055E+00,
 COMP(1,5)= 1.08847E+00, 1.11650E+00, 1.12139E+00, 1.11585E+00, 1.11056E+00,
            1.09975E+00, 1.09140E+00, 1.08463E+00, 1.07878E+00, 1.07361E+00,
            1.06904E+00, 1.06497E+00, 1.06131E+00, 1.05801E+00, 1.05502E+00,
            1.05159E+00,
 COMP(1,6)= 1.15668E+00, 1.18397E+00, 1.18506E+00, 1.17411E+00, 1.16747E+00,
            1.14972E+00, 1.13635E+00, 1.12597E+00, 1.11726E+00, 1.10958E+00,
            1.10279E+00, 1.09674E+00, 1.09133E+00, 1.08643E+00, 1.08199E+00,
            1.07647E+00,
 COMP(1,7)= 1.23084E+00, 1.25337E+00, 1.24902E+00, 1.23201E+00, 1.22470E+00,
            1.19962E+00, 1.18079E+00, 1.16663E+00, 1.15508E+00, 1.14492E+00,
            1.13598E+00, 1.12801E+00, 1.12088E+00, 1.11443E+00, 1.10858E+00,
            1.10325E+00,
 COMP(1,8)= 1.53474E+00, 1.52744E+00, 1.49709E+00, 1.45511E+00, 1.44905E+00,
            1.39544E+00, 1.35356E+00, 1.32290E+00, 1.29944E+00, 1.28017E+00,
            1.26313E+00, 1.24803E+00, 1.23450E+00, 1.22231E+00, 1.21122E+00,
            1.19328E+00,
 COMP(1,9)= 1.82195E+00, 1.78308E+00, 1.72700E+00, 1.66232E+00, 1.59409E+00,
            1.58172E+00, 1.51821E+00, 1.47049E+00, 1.43481E+00, 1.40660E+00,
            1.38213E+00, 1.36062E+00, 1.34135E+00, 1.32394E+00, 1.30817E+00,
            1.29372E+00,
NPBLAKE =     9, NTBLAKE =    16,
$END
```

MACE 155MM M203 INPUT FILE EXAMPLE

```
*****************************************************************************
*Case 1: 155MM GUN: M30A1 PROPELLANT, INERT WALL  STATION 1, CHROMIUM
*Case 2: 155MM GUN: M30A1 PROPELLANT, INERT WALL  STATION 1, GUNSTEEL
*****************************************************************************
 $MACE
C---
  AHL=.1, AHT=.05,
  EMISS=25*0.8,
  TABLTN=100460,
  NPROP(1)=2*25,
*****************************************************************************
*Case 1:
*C--- MATERAL PROPERTIRES FOR CHROME
*COND(1,1)=1.66515E-02,1.52076E-02,1.44002E-02,1.39670E-02,1.37215E-02,
*             1.35392E-02,1.33451E-02,1.31019E-02,1.28001E-02,1.24490E-02,
*             1.20689E-02,1.16848E-02,1.13214E-02,1.09988E-02,1.07301E-02,
*             1.05202E-02,1.03652E-02,1.02537E-02,1.01693E-02,1.00945E-02,
*             1.00146E-02,9.92486E-03,9.83751E-03,9.79026E-03,1.01559E-02,
*    CP(1,1)=9.67428E-02,1.06467E-01,1.12725E-01,1.16565E-01,1.18822E-01,
*             1.20145E-01,1.21025E-01,1.21820E-01,1.22775E-01,1.24045E-01,
*             1.25715E-01,1.27814E-01,1.30335E-01,1.33242E-01,1.36490E-01,
*             1.40029E-01,1.43815E-01,1.47814E-01,1.52010E-01,1.56405E-01,
*             1.61020E-01,1.65898E-01,1.71096E-01,1.76684E-01,1.89325E-01,
* RHO(1,1) = 25*4.46970E+02,
*C--- MATERAL PROPERTIRES FOR STEEL
*  COND(1,2)=5.20261E-03,5.52810E-03,5.77896E-03,5.95744E-03,6.06706E-03,
*             6.11312E-03,6.10237E-03,6.04347E-03,5.94669E-03,5.82358E-03,
*             5.68780E-03,5.55426E-03,5.43967E-03,12*5.43967E-03,
*    CP(1,2)=1.07003E-01,1.09799E-01,1.12798E-01,1.16217E-01,1.20090E-01,
*             1.24349E-01,1.28895E-01,1.33674E-01,1.38754E-01,1.44399E-01,
*             1.51141E-01,1.59865E-01,1.71873E-01,12*1.71873E-01,
* RHO(1,2) = 25*4.88800E+02,
*
*Case 2:
*C--- MATERAL PROPERTIRES FOR STEEL
*  COND(1,1)=5.20261E-03,5.52810E-03,5.77896E-03,5.95744E-03,6.06706E-03,
*             6.11312E-03,6.10237E-03,6.04347E-03,5.94669E-03,5.82358E-03,
*             5.68780E-03,5.55426E-03,5.43967E-03,12*5.43967E-03,
*    CP(1,1)=1.07003E-01,1.09799E-01,1.12798E-01,1.16217E-01,1.20090E-01,
*             1.24349E-01,1.28895E-01,1.33674E-01,1.38754E-01,1.44399E-01,
*             1.51141E-01,1.59865E-01,1.71873E-01,12*1.71873E-01,
* RHO(1,1) = 25*4.88800E+02,
*****************************************************************************
      TPROP=4.01400E+02,4.91400E+02,5.81400E+02,6.71400E+02,7.61400E+02,
            8.51400E+02,9.41400E+02,1.03140E+03,1.12140E+03,1.21140E+03,
            1.30140E+03,1.39140E+03,1.48140E+03,1.57140E+03,1.66140E+03,
            1.75140E+03,1.84140E+03,1.93140E+03,2.02140E+03,2.11140E+03,
            2.20140E+03,2.29140E+03,2.38140E+03,2.47140E+03,2.65140E+03,
  NTPROP=   25,
C--- GENERALIZED SURFACE CHEMISTRY
  ICHEM=1, TREFHS=0.0, HOCHEM=-2718., HTFORM=0., CPGAS = 1.32, CPTGAS=1.E-3,
  TREACT=6000, TDIFF=6000.0,
*****************************************************************************
*Case 1: HTFUSN = 139.8, TMELT = 3834,
*        BHDIFF = .991,
*Case 2: HTFUSN = 117, TMELT = 3258,
*        BHDIFF = 1.59,
*****************************************************************************
  CMOCH=1.000,
  TABGEN = T,
  ITABLE = 1,
C--- RADIANT HEAT FLUX INPUTS
  THTFLX=0,
  HTFLX= 0.0,
```

```
  NHTFLX=0,
C--- CONVECTIVE ENVIRONMENT
  ETAFLG=13*1,
  NTIME=     13,
  TIME=  0,  40E-4,  80E-4, 120E-4, 160E-4, 199E-4, 249E-4, 309E-4, 387E-4,
           447E-4, 600E-4, 735E-4, 891E-4,
  PRESS= 2*720, 1.46E6, 5.01E6, 3.83E6, 1.73E6, 8.35E5, 4.68E5, 2.52E5,
         8.89E4, 5.18E4, 1.87E4, 7.34E3,
  HR=  2*-2572, -370.9, -412.3, -711.8, -996.8, -1214.4, -1349.7, -1438.5,
       -1532.2, -1582.3, -1819.99, -2114.3,
  QCW= 2*108, 15264, 19440, 13536, 5472, 2880, 1000, 720, 288, 265, 43.2,
       124.4,
C--- TIME CONTROLS
  STAGE=0.0, 0.0891, PRINT= 1.E-3,
  STBLTY=2*.10, NSTAGE=2, DTMAX = 2.E-5, DTMIN = 1.E-7,
  ROUT = -2.3622, OMEGA = 1,
*******************************************************************************
*Case 1:  LMAX=40, TERROR=1, ALNGTH= 0.0366,2.2462, NODES=35,  NMTRLS=2,
*Case 2:  LMAX=40, TERROR=1, ALNGTH= 2.2462, NODES=35,  NMTRLS=1,
*******************************************************************************
  DISK=3,
  TERROR=0.5, WERROR=1.0E-6,
C--- OUTPUT AT FIXED LOCATIONS
  NFIXED=2,
  XFIXED= 0.01, 0.02,
 $END
*******************************************************************************
*Case 1:
*155MM GUN: M30A1 PROPELLANT ... REACTING WALL (3000 R) STATION 1 CHROMIUM
* $MACE
*  ITABLE = 0,
*  TREACT=3000, TDIFF=3400.0,
* $END
*155MM GUN: M30A1 PROPELLANT ... REACTING WALL (2800 R) STATION 1 CHROMIUM
* $MACE
*  TREACT=2800, TDIFF=3200.0,
* $END
*155MM GUN: M30A1 PROPELLANT ... REACTING WALL (2600 R) STATION 1 CHROMIUM
* $MACE
*  TREACT=2600, TDIFF=3000.0,
* $END
*155MM GUN: M30A1 PROPELLANT ... REACTING WALL (2400 R) STATION 1 CHROMIUM
* $MACE
*  TREACT=2400, TDIFF=3000.0,
* $END
*155MM GUN: M30A1 PROPELLANT ... REACTING WALL (2350 R) STATION 1 CHROMIUM
* $MACE
*  TREACT=2350, TDIFF=2800.0,
* $END
*155MM GUN: M30A1 PROPELLANT ... REACTING WALL (2000 R) STATION 1 CHROMIUM
* $MACE
*  TREACT=2000, TDIFF=2400.0,
* $END
*155MM GUN: M30A1 PROPELLANT ... REACTING WALL (1800 R) STATION 1 CHROMIUM
* $MACE
*  TREACT=1800, TDIFF=2200.0,
* $END
*
*Case 2:
*155MM GUN: M30A1 PROPELLANT ... REACTING WALL (1600 R) STATION 1 GUNSTEEL
* $MACE
*  ITABLE = 0,
*  TREACT=1600, TDIFF=3000.0,
* $END
*155MM GUN: M30A1 PROPELLANT ... REACTING WALL (1550 R) STATION 1 GUNSTEEL
* $MACE
```

```
*  TREACT=1550, TDIFF=3000.0,
* $END
*155MM GUN: M30A1 PROPELLANT ... REACTING WALL (1400 R) STATION 1 GUNSTEEL
* $MACE
*  TREACT=1400, TDIFF=2800.0,
* $END
*155MM GUN: M30A1 PROPELLANT ... REACTING WALL (1350 R) STATION 1 GUNSTEEL
* $MACE
*  TREACT=1350, TDIFF=2600.0,
* $END
*155MM GUN: M30A1 PROPELLANT ... REACTING WALL (1200 R) STATION 1 GUNSTEEL
* $MACE
*  TREACT=1200, TDIFF=2400.0,
* $END
*155MM GUN: M30A1 PROPELLANT ... REACTING WALL (1150 R) STATION 1 GUNSTEEL
* $MACE
*  TREACT=1150, TDIFF=2000.0,
* $END
*155MM GUN: M30A1 PROPELLANT ... REACTING WALL ( 800 R) STATION 1 GUNSTEEL
* $MACE
*  TREACT= 800, TDIFF=1600.0,
* $END
**************************************************************************
```